Coupled Enthalpic-Packing Effects on the Miscibility of Conformationally Asymmetric Polymer Blends

Chandralekha Singh† and Kenneth S. Schweizer*

Department of Materials Science and Engineering, Chemistry, and Materials Research Laboratory, University of Illinois, 1304 W. Green St, Urbana, Illinois 61801

Received September 9, 1996; Revised Manuscript Received December 19, 1996[⊗]

ABSTRACT: A systematic numerical study of a minimalist model of conformationally and interaction asymmetric model binary blends has been carried out based on a computationally convenient formulation of PRISM theory and the free energy route to the thermodynamics. Effective χ-parameters based on the correlated enthalpic contribution to the free energy of mixing are computed within a constant volume and conformationally ideal description. The model calculations are carried out for molecular parameters which span the plausible range for hydrocarbon materials such as the polyolefins. Distinct regimes of miscibility behavior are found depending on whether the conformational and interaction asymmetries reinforce or tend to compensate. The former case is the most common experimental situation, and large positive χ-parameters are predicted due to the nonadditive influence of unfavorable bare energetic interactions and local packing differences between the stiffness asymmetric species. The theory predicts many non-mean-field behaviors observed in recent experiments such as failure of naive group contribution schemes, strong deuteration swap effects for random copolymer alloys, breakdown of the random copolymer theory for the effect of copolymer composition, and the possibility of unusual temperature dependences of, and apparent entropic contribution to, the effective χ-parameter. If the conformational and interaction asymmetries tend to anticorrelate or compensate, then the theory predicts the possibility of negative χ-parameters associated with blend composition-dependent local packing rearrangements. This novel feature suggests several design strategies for achieving miscible high molecular weight polyolefin blends by rationally manipulating conformational and dispersion force properties of the polymer molecules. The blend theory is also compared with a microscopic version of a pure component-based solubility parameter theory. Overall, a remarkable agreement is found in the asymmetry reinforcement regime, but significant mixing "irregularities" can occur especially in the asymmetry compensation regime.

I. Introduction

Understanding the molecular factors which control the miscibility and phase diagrams of polymer blends is both a fascinating and complex scientific issue, and a problem of significant materials science and engineering importance. For nearly all cases of interest, the components of the blends are characterized by multiple "asymmetries" of both an energetic and molecular structure origin. Energetic, or chemical interaction, asymmetries are present at the monomer level and are associated with variable intermolecular forces (particularly attractive potentials). Structural asymmetry can arise from differences in monomer shape, size, degree of sidegroup branching, backbone persistence length ("stiffness"), etc. Such single chain structural differences can strongly influence liquid phase intermolecular packing on all length scales, an effect often described as of noncombinatorial entropic nature. However, beyond the most naive mean field theory (e.g., incompressible Flory−Huggins[1]), excess contributions to the free energy of mixing cannot generally be separated into purely entropic ("athermal") and enthalpic ("thermal") contributions.

Recently, the miscibility behavior of binary blends of polyolefins has been systematically explored experimentally.[2−10] Since polyolefins are saturated hydrocarbons, they might appear to be simple materials in the sense that the bare dispersion forces, liquid density, and other properties are nearly the same for all monomer structures. Based on Flory−Huggins mean field theory, and the fact that all polyolefins have the same chemical formula, this would imply most polyolefin blends (and diblock copolymers) are miscible. In reality, just the opposite is true, presumably due to the thermodynamic consequences of variable monomer architecture (e.g., branching) and backbone stiffness, sometimes collectively refered to as "conformational asymmetry" effects.[8,11] Whether the primary origin of polyolefin immiscibility is "nonlocal entropic" or "enthalpic" is a matter of debate among both experimentalists and theorists. On the experimental side, the Exxon/Princeton group,[2−7] Crist and co-workers,[9] and Klein and coworkers[10] have argued for the local enthalpic mechanism, and phenomenological solubility parameter schemes with some predictive ability have been successfully deduced from the data. On the other hand, Bates and co-workers[8] have suggested an entropic packing frustration mechanism associated with spatially nonlocal (correlation hole scale) considerations. Fredrickson, Bates and Liu[12] have constructed a phenomenological Gaussian field theory based on this hypothesis, which has subsequently also been derived from liquid state theory based on a random phase approximation (RPA) closure for singular repulsive forces.[13]

As motivation, and for subsequent discussion purposes, it is worthwhile to briefly summarize the primary "non-mean-field" trends which have emerged from recent experimental studies.[2−10] An incomplete list includes: (i) failure of group contribution (or bond additivity) solubility parameter schemes for estimating an effective interaction or χ-parameter,[2−9] (ii) strong deuteration swap effects on χ,[2,3,9,10] (iii) failure of mean field random copolymer theory for describing molecular

† Present address: Department of Materials Science and Engineering, and Physics, 848 Benedum Hall, University of Pittsburgh, Pittsburgh, PA 15261.

[⊗] Abstract published in *Advance ACS Abstracts,* February 1, 1997.

S0024-9297(96)01332-0 CCC: $14.00

composition effects,[2−5,9] (iv) unusual, non-mean-field temperature dependences of χ,[2−5] and (v) negative χ-parameters and heating induced phase separation in special polyolefin mixtures.[2,4] As discussed by the experimentalists, none of these effects appear understandable based on the simplest, incompressible Flory−Huggins mean field theory[1] which accounts only for the "bare" chemical interactions within a random mixing, constant volume, lattice model framework. Attempts to rationalize the blend data based on compressible "equation-of-state" theories[14] (with empirical parameters) have also not been successful.[2−5,7]

Our approach to developing a theoretical basis to understand the complex polyolefin mixing behavior has been based on Polymer Reference Interaction Site Model (PRISM) integral equation methods[15] in conjunction with coarse-grained models of polymer structure.[11,13,16−21] Since there has been a significant amount of such studies already published, we first summarize prior work to place our present study in context. For phase transitions and thermodynamic properties, PRISM theory can be applied at various levels of statistical mechanical sophistication (and implementation complexity). In addition, chain models of various levels of chemical realism can be adopted (the "coarse-graining" question). Exploration of the dependence of PRISM theory predictions on the degree of model coarse-graining allows the subtle question of what features of monomer structure are critical to the miscibility question to be addressed.[15,17] Our work has focussed on binary mixtures of homopolymers at two significantly different levels of molecular description. (1) The simplest model of a polymer as a fully flexible, infinitely thin Gaussian space curve ("thread") for which analytical results can be derived.[11,15,17−23] This model is closest in spirit to that adopted in field theoretic approaches.[24] (2) Numerical studies employing a finite thickness, semiflexible chain (SFC) model[26] which explicitly captures the transition from a locally stiff backbone to a fully flexible ideal walk on large length scales.[13,15,25] The recent version of this SFC model (referred to as "melt-calibrated") has been fine tuned such that it predicts (based on PRISM theory) chain-averaged intermolecular pair correlation functions, $g(r)$, and total cohesive energies which agree surprisingly well with both PRISM studies and computer simulations of atomistic models of one-component polyolefin melts.[17] This pure component work serves as important motivation and justification of the approach to blends we pursue in this paper. Besides the degrees of polymerization, the local, material-specific structural asymmetry of the blend enters via species-dependent effective chain aspect ratio (SFC) or statistical segment lengths (Gaussian thread).

Intermolecular interactions are modeled as pair decomposable site-site potentials consisting of a repulsive hard core plus species dependent attractive tail potentials. In the simplest model case, the spatial form of all the attractive tail potentials are taken to be the same, with a strength parameter (well depth) which obeys a geometric combining (Berthelot) relation.[11,20] In our view this is a "minimalist" model, which captures the real intrachain structure and interchain interactions in the spirit of a monomer-averaged effective homopolymer approximation. Prior (and the present) studies have been carried out at constant volume. This is the technically and computationally simplest case and would seem reasonable for polyolefins which have nearly identical melt densities and show very small excess volumes of mixing.[2,3,7] Of course, experiments are performed at constant pressure, and this can affect polyolefin phase diagrams in interesting ways.[31]

In earlier athermal and thermal blend studies, analytic PRISM predictions for the Gaussian thread model have been derived based on two distinct levels of statistical mechanical approximation: the blend molecular closure approximations[11,20] and a microscopic solubility parameter approach.[18] The purely athermal, conformationally asymmetric thread blend was found to be a miscible, nearly ideal mixture.[15,19] However, in the presence of thermal interactions (tail potentials) the structural asymmetry can strongly promote phase separation, and its influence is not separable from the interaction (chemical) asymmetries.[11,20] In particular, conformational asymmetries result in nonrandom packing, which via a correlated enthalpic mechanism are predicted in most cases to strongly destabilize homogenous phases of polyolefins. *Qualitative* agreement between the theoretical predictions (at either the blend molecular closure[20] or microscopic solubility parameter level[18]) with *most (not all)* of the puzzling non-mean-field theory observations listed above have been demonstrated.

However, several fundamental questions were avoided in the analytic PRISM work based on the idealized Gaussian thread model. These include: (a) what is the statistical mechanical basis and limitations of a solubility parameter level theory?; (b) what are the consequences of finite chain thickness and stiffness (semiflexibility) on the theoretical predictions and prior conclusions concerning the relative importance of correlated enthalpy versus noncombinatorial entropic contributions to the free energy of mixing?; and (c) what is the influence of finer structural features such as explicit chain branching, nonspherical monomer shape, and constant pressure ("equation-of-state") corrections? Some aspects of questions a and b have begun to be addressed recently both by numerical PRISM studies[16,18] and off-lattice computer simulations.[27−29] Detailed PRISM and Monte Carlo studies of athermal, stiffness asymmetric SFC blends[18,27,28] has led to the following conclusions. (i) For experimentally relevant degrees of polymerization and chain aspect ratios, the phenomenon of entropy-driven athermal phase separation does *not* occur. (ii) The purely entropic effective χ-parameters are small relative to $2/N$ (nearly ideal mixing in a thermodynamic sense) and much less important than the effect of thermal interactions (tail potentials) in the presence of local conformational asymmetry. (iii) PRISM theory is in excellent agreement with the athermal blend simulations for both the structural correlations and constant volume mixing thermodynamic properties. Very recent Monte Carlo simulations by Kumar and Weinhold[29] of stiffness-mismatched thermal blends have also qualitatively verified some of the striking non-mean-field PRISM predictions analytically derived for conformationally asymmetric Gaussian thread mixtures.[20]

On the basis of constant volume continuous space PRISM theory, Curro and co-workers[30] have recently addressed question c for an atomistically realistic model of a polyethylene and polypropylene mixture. Their results concerning the effective χ-parameter, and the relative importance of thermal versus athermal effects, are in qualitative agreement with our PRISM predictions based on the more coarse-grained models. Recent compressible lattice cluster theory (LCT) studies of polyolefin blends by Dudowicz and Freed[31] also system-

atically address question c and appear to be in qualitative accord with our PRISM-based conclusion of strong coupling of local structural asymmetry, interchain packing, and enthalpic effects. LCT also finds that the "entropic" part of χ becomes increasingly significant for more miscible systems.[31] Although there are certainly differences between the PRISM predictions based on coarse-grained models and more atomistic PRISM and LCT approaches, and coarse-grained molecular models will undoubtably fail for certain systems, the level of agreement at this time is encouraging. Besides being considerably simpler than atomistic PRISM studies from a technical point of view, since our minimalist model approach focuses on only a few key structural features within a monomer-averaged-interaction framework, it affords the possibility of obtaining rather general insights. This is most likely to occur within a homologous series of materials such as the polyolefins, and for such materials our approach may be of conceptual and molecular design value.

The specific purpose of this paper is to both describe in depth and extend the preliminary results recently published as a brief communication[16] which address questions a and b stated above. We employ the melt-calibrated SFC model,[16,17] and the simplest possible statistical mechanical and computational level of numerical PRISM theory to compute the excess free energy of mixing: thermodynamic perturbation theory or the so-called "high temperature approximation" (HTA).[32,33] This standard HTA approach to thermodynamics *assumes* that the intermolecular packing of chains is dominated by the hard core repulsive forces, a situation for which PRISM theory has been shown to be very accurate by comparison to simulations of athermal melts[34−36] and binary blends.[27,28] For the reasons discussed above and elsewhere, the (small) purely excess entropic contributions to the free energy of mixing will be ignored.[13,18,27] The numerical results are reported in the form of an effective χ-parameter arising from correlated enthalpic effects, and systematic model calculations of χ *with structural and interaction energy parameters relevant to polyolefins*[17,13,18] *and other flexible polymer alloys (e.g., dienes)* are presented. A microscopic, pure-melt based solubility parameter approach is also carried out in order to address question a above.

One of our primary conclusions is that nearly all the predictions obtained using the simpler statistical mechanical approach (microscopic melt solubility parameters[18]), or the Gaussian thread model and molecular closures,[20] remain *qualitatively* valid. Of course, quantitative modifications do emerge as expected. However, an entirely new behavior, the possibility of *negative* effective χ-parameters in the absence of any "specific attractions" between unlike homopolymer species, is predicted by the blend HTA theory. Although the relation between asymmetry parameters required for this behavior is not expected to generally occur for most polyolefin blends, it may be possible to realize in special cases and represents a novel possible mechanism for rationally designing miscible, high molecular weight polyolefin alloys. This result may also have relevance to understanding some of the "irregular" mixing behavior documented in polyolefin blends, and the surprising low temperature negative χ-parameters recently observed for polyisobutylene-containing and other saturated hydrocarbon alloys.[2,4]

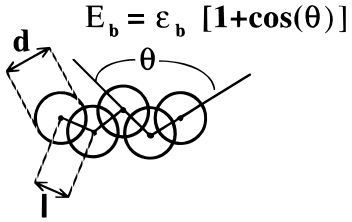

Figure 1. Schematic diagram of the overlapping semiflexible chain model. The ratio of the bond length l to the hard core diameter is chosen to be $l/d = 0.5$. The bending energy ϵ_b is changed to yield the desired chain stiffness.

We believe our results are of more general interest than for just polyolefin alloys, and they are also directly testable by modern computer simulation methods. Hence, in this paper we focus on establishing the predicted trends without a detailed discussion of how the model parameters are precisely related to specific experimental blend systems. Making such precise contact is quite involved since parameters such as the density, aspect ratio, and van der Waals attraction strengths depend not only on chemical species and coarse-graining procedure, but also implicitly on temperature. We shall pursue a detailed confrontation of our predictions with small angle neutron scattering (SANS) and cloud point data for of order 100 polyolefin blends in a forthcoming publication.[37] Here, we will only discuss how our predicted trends compare with experiments in a qualitative, or semiquantitative, manner.

The remainder of the paper is organized as follows. In Section II the SFC chain and intermolecular potential models are discussed, and the elementary aspects of PRISM theory are summarized. Thermodynamic perturbation theory, the effective blend χ-parameter, and the microscopic solubility parameter approach are discussed in Section III. Our numerical results for homopolymer blends and a simple model of random copolymer blends are presented in Sections IV and V, respectively, and qualitatively discussed in light of the host of non-mean-field experimental observations on polyolefin blends. The paper concludes with a brief summary in Section VI.

II. Model and PRISM Theory

A. Model. We consider a binary mixture of single site homopolymers labeled as A and B. As a first approximation we assume the intrachain conformation of the blend components to be ideal (blend composition independent). The discrete semiflexible chain model[38,39] is adopted; the geometry is shown in Figure 1. The total energy of the chain is given by the sum of the bending energies associated with the bond angle between three consecutive segments: $E_b = \epsilon_b(1 + cos\ \theta)$, where ϵ_b is the local bending energy. The hard core diameters and degrees of polymerization of the components are assumed to be identical for simplicity, i.e., $d_{AA} = d_{BB} = d$, and $N_A = N_B = N$. The ratio of the bond length l to the hard core diameter is chosen to be $l/d = 0.5$. This choice of l/d is motivated by both geometric considerations of the accessible surface area to volume ratio of real monomers, and by our earlier observation[17] that for appropriate choice of chain aspect ratio this overlapping semiflexible chain model can mimic the (chain-averaged) local intermolecular radial distribution functions and relative cohesive energies of hydrocarbon melts. Thus, the structural asymmetry in our minimalist model arises solely from the difference in the bending energies

of the two components $\epsilon_{b,A}$ and $\epsilon_{b,B}$. A physically relevant dimensionless measure of chain stiffness is an "aspect ratio", which we define as $\Gamma_m = \sigma_m/d$, where $(6R_{g,m}^2/N)^{1/2}$ is the effective segment length and $R_{g,m}$ is the radius-of-gyration of component m. A dimensionless measure of total liquid density is the packing fraction $\eta = (\pi/6)\,\rho d^3$, where ρ is the total site number density. For most of the present model calculations ρ, d, and Γ_m are taken to be independent of temperature and blend composition ϕ (defined as the volume fraction of A sites).

The site-site intermolecular potential between species m and m' is taken to consist of a hard core of diameter d plus a shifted Lennard−Jones attractive tail. The repulsive and attractive potentials, $u_{mm'}(r)$ and $v_{mm'}(r)$, respectively, are given by

$$u_{mm'}(r) = \infty, \qquad r < d$$
$$u_{mm'}(r) = 0, \qquad r > d \tag{2.1}$$
$$v_{mm'}(r) = 0, \qquad r < d$$

$$v_{mm'}(r) = \epsilon_{mm'}\left[\left(\frac{d}{r}\right)^{12} - 2\left(\frac{d}{r}\right)^{6}\right], \qquad r > d \tag{2.2}$$

where $\epsilon_{mm'}(r)$ is the van der Waals interaction strength between monomers m and m' at contact. Interaction asymmetry is modeled by employing the Berthelot geometric combining relation as a mimimalist description of nonpolar, van der Waals interactions:

$$\lambda^2 = \frac{\int d\vec{r}\, v_{BB}(r)}{\int d\vec{r}\, v_{AA}(r)} = \frac{\epsilon_{BB}}{\epsilon_{AA}}$$

$$\lambda = \frac{\epsilon_{AB}}{\epsilon_{AA}} \tag{2.3}$$

At this level, the energy ϵ_{AA} can be chosen to nondimensionalize the temperature, and λ^2 quantifies the bare (average) chemical interaction difference between A and B monomers. For polyolefins the interaction strengths of the methyl, methylene, and methyne groups are reasonably well known.[40] Hence, the Berthelot parameter λ can be estimated by computing a weighted arithmetic sum of the energy parameters of methyl, methylene, and methyne groups.[18,40,41] Since the A and B sites are chosen to have equal volume, such estimates should be performed on an equal (reference) volume basis e.g., a four-carbon C_4H_8 unit for polyolefins. Such an approach yields a λ for a polyethylene−polyethylethylene (PE−PEE) blend of $\approx$1.04−1.06.[17,18]

B. PRISM Theory. In Fourier space, the PRISM matrix equation[42] for a mixture of *homo*polymers, after preaveraging chain end effects,[43] is given by

$$\hat{h}_{mm'}(k) = \hat{\omega}_m(k)[\hat{C}_{mm'}(k)\hat{\omega}_{m'}(k) + \sum_{m''}\hat{C}_{mm''}(k)\rho_{m''}\,\hat{h}_{m''m'}(k)] \tag{2.4}$$

where ρ_m is the site number density of species m, $\omega_m(r)$ is the intramolecular pair correlation function of species m, $h_{mm'}(r) = g_{mm'}(r) - 1$, where $g_{mm'}(r)$ is the chain-averaged intermolecular pair correlation function between interaction sites of species m and m', and $C_{mm'}(r)$ is the corresponding intermolecular site−site direct correlation function. The direct correlation functions can be regarded as renormalized potentials which include many body correlation effects.[32] The single chain structure factors $\hat{\omega}_m(k)$ are calculated using the discrete Koyama model[44] for semiflexible chains by a procedure identical to that used by Honnell *et al.*[26,45] The partial collective structure factors are given by

$$\hat{S}_{mm'}(k) = \rho_m\hat{\omega}_m(k)\delta_{mm'} + \rho_m\rho_{m'}\hat{h}_{mm'}(k) \tag{2.5}$$

Implementation of the theory requires an approximate closure relation. Hard core impenetrability corresponds to $h_{mm'}(r) = -1$ for $r < d$. Outside the hard core we employ the standard site-site Percus−Yevick closure approximation[33]

$$C_{mm'}(r) = 0, \qquad r > d \tag{2.6}$$

In contrast to a literal incompressibility approximation, due to the structural asymmetry the three athermal blend structure factors $\hat{S}_{mm'}(r)$ and the hard core direct correlation function $\hat{C}_{mm'}(r)$ *must* all be different in general.[20] Moreover, consistent with the fact that we shall employ the free energy route perturbation method to calculate the mixing thermodynamic properties, only the repulsive ("athermal") part of the potential in eq 2.2 is taken into account in the PRISM calculations of interchain structure. Direct tests of this simplification based on using PRISM with molecular closures have shown that the perturbation of structurally asymmetric blend packing correlations by the attractive tail potentials is weak for $N \approx 500-5000$ unit polymers.[46,47] The PRISM equations along with the closure condition are solved numerically via the Picard iteration scheme using the fast Fourier transform as described in ref 25.

III. Effective χ-Parameter and Phase Separation

A. General Approach. The free energy of mixing per repeat unit (site) in units of thermal energy is given by:[13,18,30,32]

$$\beta\Delta F = \left\{\frac{\phi\ln(\phi)}{N} + \frac{(1-\phi)\ln(1-\phi)}{N}\right\} + \beta F_b^{(0)} + \left\{\frac{\beta}{2\rho}\sum_{mm'}\rho_m\rho_{m'}\int d\vec{r}\, v_{mm'}(r)\int_0^1 d\lambda\, g^{\lambda}_{mm'}(r)\right\} - \{\phi\beta\delta F_{A,Melt} + (1-\phi)\beta\delta F_{B,Melt}\} \tag{3.1}$$

where $\rho_A = \phi\rho$, $\rho_B = (1-\phi)\,\rho$, ρ = total site number density, $\beta = (k_BT)^{-1}$, and single chain conformational contributions are absent due to the assumed ideality of $\omega_m(r)$. The first term in eq 3.1 is the ideal combinatorial entropy of mixing and is denoted by $\beta\Delta F_{id}$. The second term is the excess noncombinatorial free energy of the blend associated with the repulsive hard core interactions. It represents the excess entropy of the hypothetical athermal blend. The third term is the blend enthalpic free energy, i.e., the blend free energy associated with the attractive branch of the interchain potentials. This contribution takes the form of a "charging" integral with the charging parameter λ varying from $\lambda = 0$ (no attractive potential) to $\lambda = 1$ (full attractive potential). The last term is the appropriately weighted pure component excess free energy contribution which is linear in ϕ. For the blend enthalpic free energy the high temperature, perturbative approximation is obtained by assuming that

$$g^{(\lambda)}_{mm'}(r;\lambda v_{mm'}) = g^0_{mm'}(r) \tag{3.2}$$

where $g^0_{mm'}$ are the *composition-dependent* pair correlation functions in the athermal repulsive force reference blend. We note that since the van der Waals attractions $v_{mm'}(r)$ are spatially local, the blend enthalpy is strongly dependent on the *local* interchain packing which is very sensitive to the local conformation or stiffness of the A and B chains.

Within the free energy route to thermodynamics a single effective χ-parameter is defined in terms of the excess free energy of mixing, $\Delta F_{exc} = \Delta F - \Delta F_{id}$, via the standard second compositional derivative relation:

$$\chi = -\frac{1}{2}\frac{\partial^2 \beta \Delta F_{exc}}{\partial \phi^2}$$

$$= -\frac{1}{2}\frac{\partial^2}{\partial \phi^2}\left\{\beta F_b^{(0)} + \frac{\beta}{2\rho}\sum_{m m'}\rho_m \rho_{m'}\int d\vec{r}\, v_{mm'}(r) g^0_{mm'}(r)\right\}$$

$$= -\frac{1}{2}\frac{\partial^2 \beta (F_b^{(0)} + F_{th})}{\partial \phi^2} = \chi_{ath} + \chi_{th} \qquad (3.3)$$

The condition for liquid−liquid spinodal phase separation, and corresponding χ-parameter χ_S, is given by

$$2\chi_S N\phi(1-\phi) = 1 \qquad (3.4)$$

Equation 3.3 shows that the χ-parameter can be formally separated into an athermal or entropic contribution, χ_{ath}, associated with the (reference) athermal blend, and an enthalpic contribution, χ_{th}, due to the attractive part of the interaction potential. Such a labeling is somewhat misleading since even the entropic term is temperature dependent due to the implicit temperature dependence of the effective site hard core diameter, density, and intra-molecular structure. In addition, the enthalpic contribution is strongly influenced by local packing correlations in the athermal reference system, which is a noncombinatorial or interaction entropic effect. We note that the last term in eq 3.1 involving the excess melt free energy is not relevant for determining the spinodal instability nor effective χ-parameter since $F_{m,Melt}$ in the pure melt is independent of composition. As discussed in the Introduction, our prior studies[13,27] suggest that the athermal χ-parameter generally obeys $\chi_{ath} \ll \chi_S$ for the parameters appropriate for most flexible polymers, and the enthalpic contribution is larger by at least 1 order of magnitude, i.e., $\chi_{th} \gg \chi_{ath}$. Thus, we concentrate solely on the effective enthalpic χ-parameter χ_{th}.

The terms arising from taking the second partial derivative of F_{th} for calculating the enthalpic χ-parameter χ_{th} can in general be separated into three categories: terms where $\rho_m \rho_{m'}$ has been differentiated twice, terms where $g^0_{mm'}(r)$ is differentiated twice, and terms where each is differentiated once. If the $g^0_{mm'}(r)$ functions were independent of composition, only the first contribution to χ_{th} survives:

$$\chi_{th} \to \chi_B = \frac{\rho\beta}{2}\int d\vec{r}\,[v_{AA}(r)\, g^0_{AA}(r) + v_{BB}(r) g^0_{BB}(r) - 2v_{AB}(r)\, g^0_{AB}(r)] \qquad (3.5)$$

Note that χ_B has the arithmetic difference or exchange energy form of incompressible Flory theory but corrected by the local contact probabilities. If literal random mixing is assumed, $g^0_{mm}(r) = 1$ for $r > d$, then χ_B reduces to the Flory form

$$\chi_0 = \frac{\rho\beta}{2}\int d\vec{r}\,[v_{AA}(r) + v_{BB}(r) - 2v_{AB}(r)] \to (10\,\pi/9)\rho d^3 \beta \epsilon_{AA}(\lambda - 1)^2 \qquad (3.6)$$

For saturated polyolefin blends the interaction strength between the blend components is very similar since both components are composed of methyl, methylene, and methyne groups. If all the interaction strengths are assumed to be equal to $v(r)$, then $\chi_0 \to 0$ but χ_B is given by

$$\chi_B = \frac{\rho\beta}{2}\int d\vec{r}\, v(r)\Delta g^0(r)$$

$$\Delta g^0(r) = g^0_{AA}(r) + g^0_{BB}(r) - 2g^0_{AB}(r) \qquad (3.7)$$

where $\Delta g^0(r)$ describes, in a spatially resolved manner, nonrandom mixing or physical clustering tendency in the athermal reference blend. Since the athermal blend pair correlations are ϕ-dependent, eqs 3.5 and 3.7 are not generally adequate. The corrections are due to ϕ-dependent changes in local blend packing, the thermodynamic consequences of which will be denoted as

$$\Delta\chi_{th} = \chi_{th} - \chi_B \qquad (3.8)$$

The Picard iteration procedure is utilized to numerically obtain $g^0_{mm'}(r)$. Convergence to a high accuracy with an error tolerance $\sim 10^{-11}$ is achieved. The required partial second derivative in eq 3.3 is then taken numerically by fitting $F_{th}(\phi)$ to a polynomial. The convergence of the Picard iteration to a high accuracy is important since the χ-parameter is generally a small difference of large numbers.

The treatment of the athermal hard core blend as the reference system and the attractive tail potential at the level of perturbation theory greatly increases the efficiency (speed) of our χ-parameter calculations relative to numerical studies with a molecular closure treatment of the attractions. Once the pair correlation functions are calculated from an athermal blend calculation, the enthalpic χ-parameter χ_{th} can be computed for any value of interaction asymmetry using eq 3.3 without the need for numerical solution of the nonlinear PRISM equations for every temperature and $v_{mm'}(r)$ choice of interest.

B. Microscopic Solubility Parameter Theory. We shall also calculate the enthalpic χ-parameter based on a microscopic version of the Hildebrand solubility parameter theory. The required interchain pair correlation functions of the pure component melts, $g^{(0,Melt)}_{mm}(r)$, are calculated numerically using the same SFC model employed in the blend. The approximations involved in obtaining the Hildebrand or solubility parameter theory are well known and have been listed in ref 18. The resulting expression for the χ-parameter is given by

$$\chi_H = \frac{1}{2}\beta(\delta_A - \delta_B)^2$$

$$\delta_m^2 = -\rho\int d\vec{r}\, v_{mm}(r)\, g^{0,M}_{mm}(r) \qquad (3.9)$$

where δ_m^2 is the cohesive energy, and δ_m is a corresponding solubility parameter of species m. We note that from a theoretical perspective eq 3.9 can be quite

subtle since the bare energetics and interchain packing correlations of species m enter in a nonseparable, multiplicative fashion.[18] The packing correlation aspect depends on monomer and conformational structure (e.g., backbone stiffness) and is *absent* in standard empirical solubility parameter approaches based on atomic or bond additivity schemes.[40,41] Analytical results for χ_H based on the Gaussian thread model have been previously derived[18] and will be contrasted with numerical SFC model predictions in Sections IV and V.

Graessley, Lohse, and co-workers[2−7] have extracted the solubility parameters for many polyolefins by measuring the χ-parameters of binary blends and assuming that eq 3.9 holds. The solubility parameters obtained in this manner are usually (but not always) in reasonable agreement with those obtained by the direct PVT measurements on the pure one component melt.[2] Since the experimental χ-parameter is measured for the blend, but eq 3.9 is used to extract δ_m, the implicit assumption in this approach is the validity of a geometric combining relation

$$\int d\vec{r}\, v_{AB}(r) g^0_{AB}(r) = \sqrt{\left[\int d\vec{r}\, v_{AA}(r) g^0_{AA}(r) \int d\vec{r}\, v_{BB}(r)\, g^0_{BB}(r)\right]} \quad (3.10)$$

where $g^0_{mm}(r)$ is the pair correlation function of species m *in the blend*. The latter is implicitly assumed to be ϕ-independent and pure-component-like in nature.

IV. Model Calculations: Homopolymer Blends

In this section we present numerical results for the reduced effective thermal χ-parameter, $\chi_{th}/(\beta\epsilon_{AA})$, for homopolymer binary AB blends. We define species B to be the stiffer chain ($\Gamma_B > \Gamma_A$) and refer to the A species as the "flexible" component. We have three general goals. (1) Assess the general trends in the miscibility of semiflexible polymers as a function of the average blend aspect ratio ($\bar{\Gamma} = (\Gamma_A + \Gamma_B)/2$), the conformational or stiffness asymmetry quantified as $\Delta\Gamma = \Gamma_B - \Gamma_A$ or $\gamma = \Gamma_B/\Gamma_A$, temperature, blend composition ϕ, the level of deuteration, and chemical interaction mismatch (λ parameter defined in eq 2.3) using the full-blend theory for χ_{th}. (2) Comparison of the thermal χ-parameter predictions using the full-blend theory (χ_{th}) with those obtained using the numerical solubility parameter theory (χ_H) in order to identify the conditions under which the pure component based approach works reasonably well and when it fails. (3) Test the reliability of the Gaussian thread model solubility parameter theory derived in ref 18 with regard to its prediction of the dependence of the χ-parameter on the structural and interaction asymmetry variables.

The calculations are performed using the overlapping semiflexible chain (SFC) model with the aspect ratios of the components varying over a range relevant to polyolefins, polydienes, and many other polymers $\bar{\Gamma} \approx 0.8-1.4$.[17,18] The bending energy of the SFC is adjusted to yield the desired aspect ratio. Upon the basis of a melt level calibration scheme, we have shown earlier[17,18] that the appropriate aspect ratio for polyethylene at $T \sim 400$ K is $\Gamma \approx 1.2$. Experiments[2,3,5,7] and simulations[48] have shown that the increase in the branch content of polyolefins generally reduces the characteristic ratio and increases chain thickness, and hence the effective aspect ratio is smaller so that the chains are effectively more "flexible" and pack less tightly. Thus, polyolefins which have branches have a smaller Γ than that for PE (for example, $\Gamma \approx 1$ for PEE and 1.1 for PEP.[17]). For quantitative, system-specific studies the optimal value of Γ for other polymers can be obtained by ensuring that the ratio of the pure melt solubility parameters of the blend components conforms to the experimental value.[17,18] By matching the solubility parameters obtained using the pure melt level SFC calculations with the experimentally deduced values, the Γ for most polyolefin blends is found to be in the range $\Gamma = 0.9-1.3$ consistent with apriori estimates based on known conformational properties and monomer volumes.[17,18] As Γ decreases, both the local intermolecular pair correlation function and the solubility parameter decrease. In fact, the dependence of solubility parameter on the chain aspect ratio observed experimentally for polyolefins[7] is quite similar to that obtained using the PRISM theory.[17,18,49] Typical values of λ based on molar attraction constant tables[40] fall in the range $1 < \lambda \leq 1.08$ for olefins, with the larger value corresponding to monomers with a very high CH_3 group content (branches). We emphasize that once the values of λ and Γ are determined by the above pure melt level calibration procedure,[17,18] the blend calculations could be performed *without adjusting* any parameters.

Unless noted otherwise, all the calculations presented are for a degree of polymerization $N = 2000$, a reduced total site density of $\rho d^3 = 1.375$, and an equimolar composition $\phi = 0.5$. The reduced density was chosen so that compressible PRISM theory for a PE-like melt reproduces the experimental density fluctuation strength $\hat{S}(0) = \rho k_B T \kappa_T \approx 0.25$ at $T = 430$ K where κ_T is the melt isothermal compressibility.[17] Since we are considering only the enthalpic component of the χ-parameter, the N-dependence of χ_{th} or χ_H is *very* weak, and $N = 2000$ represents essentially the asymptotic long chain limiting behavior. We have also found that χ_{th} is a weak function of blend composition, and for this reason we focus on the $\phi = 0.5$ case (but this is *not* the critical composition). The nature of the weak ϕ-dependence will be briefly discussed. The fact that in SANS measurements a significant ϕ-dependence (and often N dependence) of the extracted χ-parameter is sometimes observed in the "compositional wings" region is due to factors we believe are unrelated to the constant volume, free-energy-based thermodynamic approach utilized here. Finally, we note that at room temperature the quantity $\beta\epsilon_{AA}$ for our model is of order unity based on a four-carbon C_4H_8 repeat unit[17,18]

A. Interchain Pair Correlation Functions. Equation 3.3 shows that the local chain structure characterized by the athermal $g_{MM'}(r)$ play a central role in blend thermodynamics for structurally asymmetric blends. In Figure 2a we present a representative example of PRISM predictions for the athermal $g_{MM'}(r)$ in the blend and the corresponding $g_{MM}(r)$ in the pure athermal melt for the case $\Gamma_A = 0.85$ ("flexible" chain) and $\Gamma_B = 1.15$ ("stiff" chain). The stiff chain packs more tightly in the sense that $g_{BB}(r) > g_{AA}(r)$. Contrary to the results of the tangent SFC model of ref 13, the pair correlation function in the pure-melt is higher than that in the blend for the stiff chains, while the opposite is true for the flexible component. In other words, from a packing perspective the stiff chains appear to be less stiff and the flexible chains less flexible upon blending. Despite the nonuniversal dependence of subtle details of the melt and blend $g_{MM'}(r)$ on the ratio of the bond length to the hard core diameter, the enthalpic χ-parameter always appears to dominate over the entropic χ-param-

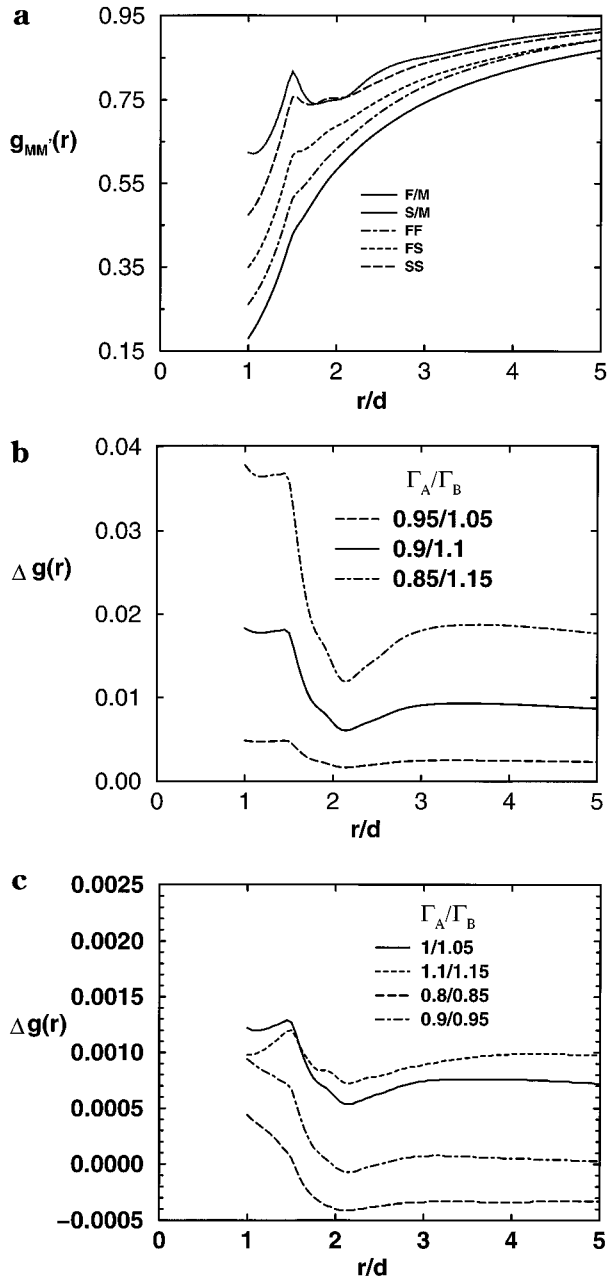

Figure 2. (a) Intermolecular site-site pair correlation functions for $\Gamma = 0.85$ (F) and 1.15 (S) chains in a 50/50 blend and their respective melts (M). (b) Intermolecular pairing function $\Delta g(r)$ for the four indicated choices of aspect ratios chosen such that the difference in the aspect ratios $\Delta\Gamma$ is constant. (c) Intermolecular pairing function $\Delta g(r)$ defined in the text for the three indicated choices of aspect ratios chosen such that the average aspect ratio $\bar{\Gamma}$ is constant.

eter for flexible polymers independent of the l/d ratio.[13]

Unlike the Flory−Huggins theory which effectively assumes $g_{MM'}(r)$ and random mixing, the deviation from random mixing or physical clustering as characterized by $\Delta g^0(r) = g^0_{AA}(r) + g^0_{BB}(r) - 2g^0_{AB}(r)$ is important for understanding correlated enthalpic effects on the blend miscibility. Apart from the term involving $\Delta g^0(r)$ in χ_{th} in eq 3.3, other terms that contribute to the χ-parameter involve taking compositional derivatives of the pair correlation functions as will be discussed in Section IV B. Examples of the athermal $\Delta g(r)$ for various aspect ratio mismatches $\Delta\Gamma = \Gamma_B - \Gamma_A$ and a fixed average aspect ratio $\bar{\Gamma} + (\Gamma_A + \Gamma_B)/2$ are shown in Figure 2b. The function $\Delta g(r)$ is relatively small, but always positive for the cases shown, indicating a packing driven preference for clustering of like monomer species. As seen from eqs 3.3−3.7, a positive $\Delta g(r)$ can induce a positive contribution to χ_{th} or χ_B thereby favoring phase separation *even if* the bare Flory $\chi_0 = 0$.[20] The deviation from random mixing increases as $\Delta\Gamma$ increases, as expected since packing frustration increases as aspect ratio mismatch increases. Figure 2c plots $\Delta g(r)$ for various $\bar{\Gamma}$ and a fixed $\Delta\Gamma = 0.05$. As $\bar{\Gamma}$ increases, $\Delta g(r)$ initially increases monotonically but there is a decrease in $\Delta g(r)$ near the contact going from $\bar{\Gamma} = 1.025$ to 1.125. Such non-universality aspects of local packing correlations play an important role in understanding the experimentally observed random copolymer effect to be discussed later.

Finally, we note that the composition dependence of the interchain pair correlation function is rather weak. In Figures 3a and 3b we plot the athermal $g(r)$'s for various compositions along with the pure melt values for a blend characterized by $\Gamma_A/\Gamma_B = 1.07/1.2$ which crudely mimics a polypropylene/polyethylene blend.[37] Although there is some change in the local $g(r)$'s as a function of ϕ, the overall change with composition is rather small. In both cases the deviations of the blend correlations from their corresponding pure melt behavior increase monotonically upon dilution by the other species, and a sign change occurs at $r \approx d + l$. The sensitivity of the stiff and flexible packing correlations to ϕ is comparable. Figure 3c plots $\Delta g(r)$ for various composition of the same blend, and deviations from random mixing of the order of a percent are found.

B. Effective Thermal χ-Parameter. In Figures 4a and 4b we plot examples of our calculations of the reduced thermal χ-parameter, $\chi_{th}/(\beta\epsilon_{AA})$, as a function of the chemical interaction mismatch variable λ for several blends characterized by different Γ_A and Γ_B ($\bar{\Gamma}$ and/or $\Delta\Gamma$ differ for various cases) using both the full blend eq 3.3 and the solubility parameter theory of eq 3.9. The χ-parameter is found to be a *non*monotonic function of λ with the smallest value (maximum miscibility) occurring at a value of λ which depends on the aspect ratios of the components. This non-monotonicity arises from the nonadditivity of the thermodynamic consequences of the structural and interaction asymmetry of the blend components.[20] The minima of the curve, or the maximum blend miscibility, occurs in the region where the two asymmetries tend to compensate each other, i.e. if the stiffer, more tightly packing blend component is more weakly interacting ($\lambda = (\epsilon_{BB}/\epsilon_{AA})^{1/2}$ and $\gamma = \Gamma_B/\Gamma_A > 1$). In the full blend theory χ_{th} near the minima can be positive or *negative* depending on the choice of parameters, while in the solubility parameter theory the minima of χ_H always occurs at zero since the χ-parameter is a perfect square as given by eq 3.9. Thus, *at the constant volume* level the full-blend theory predicts negative χ-parameters are possible (for subtle packing reasons) even in the absence of any "specific A−B interaction". For some aspect ratio choices which are suitable for flexible polymers, the negative χ-parameter near the minima can be of order -10^{-2}, a surprisingly large absolute magnitude but comparable to that recently observed at low temperatures in certain polyisobutylene and random PE/PEE copolymer blends[2−4] and mixtures of polypropylene and highly branched random olefins.[50] Of course, such large negative χ-parameters are rarely observed in polyolefins. We believe this is because the interaction asymmetry parameters for most polyolefins do not lie in the compensation

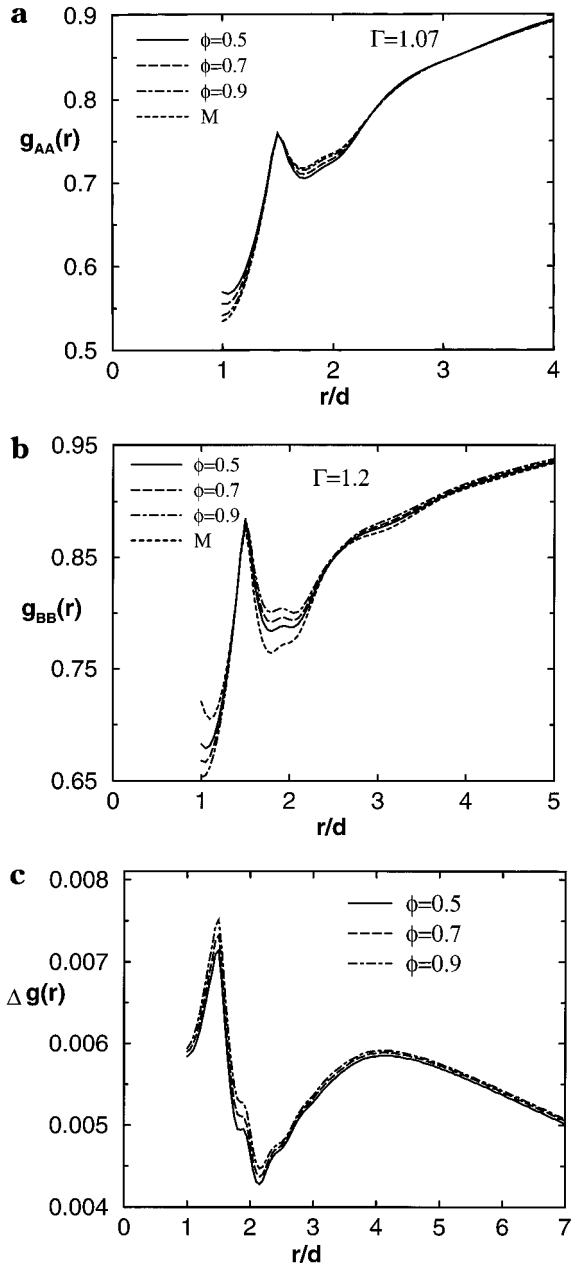

Figure 3. (a) Intermolecular site−site pair correlation functions for a pure melt of $\Gamma_A = 1.07$ and for the $\Gamma_A = 1.07$ component of blends with $\Gamma_A/\Gamma_B = 1.07/1.2$ and three different compositions $\phi = \phi_A = 0.5$, 0.7, and 0.9. (b) Intermolecular site−site pair correlation functions for a pure melt of $\Gamma_B = 1.2$ and for the $\Gamma_B = 1.2$ component of the blends with $\Gamma_A/\Gamma_B = 1.07/1.2$ and for three different compositions $\phi_A = 0.5$, 0.7, and 0.9. (c) Intermolecular pairing function $\Delta g(r)$ for three choices of blend composition and $\Gamma_A/\Gamma_B = 1.07/1.2$.

region. That is, chain branching reduces *both* the aspect ratio and van der Waals attraction so the blend is in the "asymmetry reinforcement regime" ($\gamma > 1$, $\lambda > 1$). We also note that although negative χ-parameters can emerge from classical mean field random copolymer theory[41] by suitable choice of empirical χ-parameters, the origin of $\chi_{th} < 0$ in our work is very different. It arises within an effective *homo*polymer model due to composition-dependent nonrandom packing correlations.

Even in the region where the structural and interaction asymmetries compete with each other to give a negative χ-parameter within the full blend approach, the χ_{th} and χ_H vs λ curves follow each other reasonably well. For example, for a given $\bar{\Gamma}$ and $\Delta\Gamma$ even though

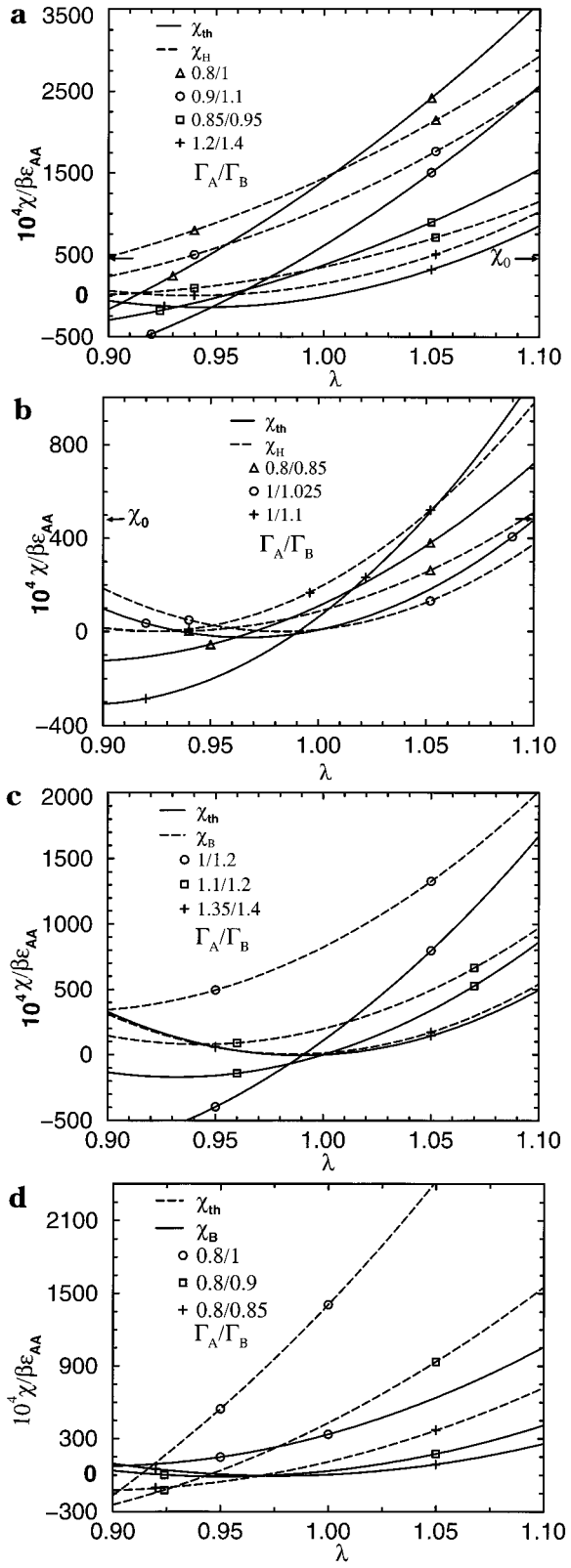

Figure 4. (a) Calculated blend (solid line) and solubility parameter (dashed line) χ- parameters in units of the reduced thermal energy as a function of the chemical asymmetry variable for four cases of structural asymmetry ($\Gamma_A/\Gamma_B = 0.8/1$, 0.9/1, 0.85/0.95, and 1.2/1.4). The symbols attached to the curves are guides to the eye for identifying the various cases. The arrow labeled χ_0 shows the mean field Flory prediction (see text) for $\lambda = 0.9$ and 1.1. (b) Same as Figure 4a but for three different cases of (weaker) structural asymmetry. (c) Same format as Figures 4a and b, but a comparison of the full blend prediction, χ_{th}, with χ_B defined in eq 3.5. (d) Same as Figure 4c, but for three different choices of structural asymmetry.

the magnitude of the χ-parameter at the minima may be rather different for the two theories, the minima occurs at approximately the same value of λ. Close examination shows that the value of λ at the minima using the full blend theory is usually smaller than that using the microscopic solubility parameter theory. Also, if $\Delta\Gamma$ is held fixed, the χ-parameter at the minima is lower for blends with lower $\bar{\Gamma}$ (within the full blend theory), and the λ required to achieve the minima is smaller (within both theories) for blends with lower $\bar{\Gamma}$.

Most polyolefin blends are in the asymmetry reinforcement regime ($\lambda > 1$ and $\gamma > 1$) which results in positive (often large) χ-parameters. For typical polyolefin blends where $\Delta\Gamma \leq 0.2$ and $\lambda \sim 1.01-1.05$, the theory predicts $\chi_{th}/(\beta\epsilon_{AA})$ in the range $\sim 0.01-0.25$. Since for $T = 300-500$ K the parameter $\beta\epsilon_{AA}$ is of order unity on a four-carbon basis,[17,18] the predicted absolute magnitudes of the χ-parameter are in the correct range measured experimentally.[2-9] As expected, the χ-parameter in the asymmetry reinforcement region typically increases with increase in aspect ratio mismatch $\Delta\Gamma = \Gamma_B - \Gamma_A$ for a fixed $\bar{\Gamma}$.

Except for the cases where the χ-parameter for the full blend theory is negative, χ_H and χ_{th} typically agree with each other to within a factor two for the whole range of λ considered. This rather surprising level of agreement provides some fundamental theoretical support for the usefulness of *microscopic* solubility parameter theory for nonpolar, high polymer blends. The differences between χ_H and χ_{th} can perhaps be interpreted as "irregular" mixing corrections which *can be of either sign*. For large values of λ, χ_H is typically larger than χ_{th}, but for some value of λ the two curves cross each other. The λ at which this crossing occurs depends sensitively on the aspect ratios of the blend and can occur before, after, or close to $\lambda = 1$. For example, for three different blends with aspect ratios $\Gamma_A/\Gamma_B = 0.9/1.1$, $1/1.025$, and $0.8/0.85$, the χ_{th} vs λ curves for the two theories cross each other around $\lambda = 1.09$, 1.0 and 0.986 where the values of the reduced χ-prameters are approximately 0.23, 0.0008, and 0.005, respectively. For $\Gamma_A/\Gamma_B = 1.2/1.4$ the curves for χ_H and χ_B do not cross and appear to be parallel over the whole range of λ shown and χ_H is always larger that χ_B. Also, for this choice of Γ_A/Γ_B the χ-parameter using the full blend theory is negative in the intermediate range of λ close to 1. The curvature, or the rate of change, of the χ-parameter at the minima is a function of the aspect ratios of the blend components and for a fixed λ the curvatures are different for blends with different Γ_A/Γ_B. Comparing various curves we find that for a fixed λ and $\Delta\Gamma$ the χ-parameter is lower for smaller $\bar{\Gamma}$ and for a fixed $\lambda > 1$ the χ-parameter is typically larger for larger $\Delta\Gamma$. Both trends are consistent with the packing correlations and local clustering shown in Figure 2. Moreover, over the range of λ considered in Figures 4a and 4b the χ_{th} curves for different blends also cross each other.

To compare with mean field Flory−Huggins (FH) theory recall that its prediction for the χ-parameter (see eq 3.6) is independent of the chain microstructure and depends only on the bare interaction asymmetry parameter as $\chi_0 \propto (\lambda - 1)^2$. Thus, χ_0 is a symmetric parabola centered around $\lambda = 1$ and $\chi_0 = 0$. It increases to a value of $10^4\chi_0/(\beta\epsilon_{AA}) \sim 475$ at $\lambda = 0.9$ and 1.1. *PRISM predictions for* χ_H and χ_{th} can be either larger or smaller than the mean field χ_0 value. However, for the asymmetry reinforcement parameter regime of primary relevance to polyolefins, χ_B and χ_H are *much larger* than χ_0, i.e., local conformational asymmetry strongly *de*stabilizes the mixed phase. Also, since the structural asymmetry of the chains competes with the interaction asymmetry to give the miscibility window in Figures 4a and 4b, PRISM predicts that the minima that usually occurs for $\lambda < 1$, and χ_{th} at $\lambda = 1$, is typically nonzero for most blends. The asymmetry of either χ_{th} or χ_H about $\lambda = 1$ emphasizes the nonadditivity of the structural and interaction asymmetries which gives rise to several novel, experimentally observable non-mean-field phenomena which we discuss in the next section.

In order to gain more insight into the origin of the predicted trends in Figures 4a and 4b, we compare in Figures 4c and 4d the full enthalpic χ-parameter χ_{th} given in eq 3.3 with the "Flory-like" correlated exchange energy contribution, χ_B defined in eq 3.5. The difference between these two χ-parameters is $\Delta\chi$ of eq 3.8, which is nonzero only because of the ϕ-dependence of the athermal blend packing correlations. Depending upon the structural asymmetries of the components, χ_B may be significantly different from χ_{th} for some range of λ. The most striking feature is that it appears $\chi_B > 0$ always. Thus, the emergence of a $\chi_{th} < 0$ in the "asymmetry compensation" regime is due to the stabilizing influence of the ϕ-dependent local packing rearrangements.

There are several more detailed trends deducable from Figures 4c and 4d. For small values of λ and a fixed Γ_A/Γ_B, χ_B is typically larger than χ_{th}, but there is a crossing of the two curves at some λ which can be smaller or larger than $\lambda = 1$ depending on the chain stiffness. After the crossing of the curves $\chi_{th} > \chi_B$ suggesting a greater destabilization of the blend in the presence of the terms involving the compositional derivatives of $g(r)$, while before the crossing of the two curves the term involving the composition dependence of $g(r)$ has a stabilizing effect on the miscibility properties. Figures 4c and 4d also clearly demonstrate that for parameters relevant for polyolefin blends the effect of the composition dependence of $g(r)$ on miscibility cannot be ignored for most cases. We find, however, for blends with relatively large average aspect ratios $\bar{\Gamma}$, that if the difference in the aspect ratios $\Delta\Gamma$ is not large the composition dependence of $g(r)$ may not make a significant contribution to the χ-parameter. An example of this is the plots for $\Gamma_A/\Gamma_B = 1.35/1.4$ where χ_B and χ_{th} are not very different for the whole range of λ.

Representative results for the composition dependence of χ_{th} of blends characterized by different values of Γ_A/Γ_B and λ are listed in Table 1. We find that for all of the blends with significantly different aspect ratios and $\lambda \neq 1$ chemical asymmetries, that the composition dependence of χ_{th} is usually remarkably weak. Similar behavior is found from LCT studies of polyolefin blends.[31] However, if χ_{th} is relatively small (as in the case of $\Gamma_A/\Gamma_B = 1.1/1.2$ and $\lambda = 1$), changing the blend composition can result in a sign change of χ_{th}. A somewhat enhanced ϕ-dependence is found for cases where $\chi \ll 0$. Since the origin of the latter behavior is ϕ-dependent structural changes ($\Delta\chi_{th}$ in eq 3.8), this is perhaps not surprising. We note that the exact value of χ_{th}, especially in the compositional wings far away from $\phi = 0.5$, is sensitive to the fitting procedure, i.e., the order of polynomial to which the free energy of mixing is fitted before numerical differentiation.

The generally weak dependence of χ_{th} on composition suggests the enthalpy of mixing, $\Delta H_{mix}(\phi)$, is nearly a

Table 1. Model Calculations of the Composition Dependence of $\chi_{th}/(\beta\epsilon_{AA})$ for Various Blends Characterized by Different Γ_A/Γ_B and Chemical Asymmetry Parameters λ. Results Are Presented for Three Different Volume Fractions of the A (flexible) Species ϕ = 0.2, 0.5, and 0.8

	$10^4\,\chi_{th}/(\beta\epsilon_{AA})$		
λ	$\phi_A = 0.2$	$\phi_A = 0.5$	$\phi_A = 0.8$
	$\Gamma_A/\Gamma_B = 1.1/1.2$		
1	4.25	−0.39	−5.82
1.1	858.45	862.15	866.48
0.9	−108.53	−132.8	−158.5
	$\Gamma_A/\Gamma_B = 1/1.2$		
1	145.1	107.49	50.76
1.1	1658.73	1673.25	1685.48
0.9	−592.46	−712.8	−871.45
	$\Gamma_A/\Gamma_B = 1.35/1.4$		
1	−0.372	−0.375	−0.378
1.1	485.5	486.6	487.9
0.9	317.6	319.0	320.64
	$\Gamma_A/\Gamma_B = 0.8/0.9$		
1	438.4	429.5	418.9
1.1	1572.9	1553.0	1415.8
0.9	−228.0	−241.07	−255.22
	$\Gamma_A/\Gamma_B = 0.8/1$		
1	1402.4	1407.2	1400.6
1.1	3609.8	3550.3	3455.5
0.9	−125.4	−159.0	−196.9

quadratic function of ϕ. As an empirical test of this idea we computed another χ-parameter defined as $\chi_{enth} = \Delta H_{mix}/(\phi(1-\phi))$ and compared it to our results for $\chi_{th} = -(1/2)\,\partial^2 H_{blend}/\partial\phi^2$. For $\phi = 1/2$ and a range of model system parameters, we found remarkably similar values from the two very different calculations. The equality $\chi_{th} = \chi_{enth}$ can only rigorously hold if either a random mixing law applies: $g^0_{MM'}(r;\phi) = g^0_{MM,melt}(r) = g^0(r)$, or the conditions required for a solubility parameter approach to be rigorous (as discussed in Section III B) were exact. Of course, neither of these conditions applies rigorously, but nevertheless our computed χ_{th} appear to be very strongly correlated with ΔH_{mix} for $\phi = 0.5$. A few studies were also carried out which compared the ϕ-dependence of χ_{th} and χ_{enth}. For systems which displayed very little ϕ-dependence of χ there was again good agreement between the two distinct interaction parameters.

We note that our finding of a weak ϕ-dependence of χ_{enth} based on PRISM theory at the constant volume HTA free energy route level has also been found by Rajasekaran and co-workers[51] for an *atomistic* model of the polyethylene/polypropylene blend. In addition, *negative* values of χ_{enth} have also been found[52] for the atomistic PE/PP blend model if an effective λ parameter is chosen to be sufficiently less than unity and hence in the "asymmetry compensation" parameter regime. The qualitative agreement between PRISM thermodynamic predictions for coarse-grained and atomistically detailed chain models for the novel asymmetry compensation and negative χ-parameter phenomenon is noteworthy.

Finally, we note that the chain length dependence of both χ_{th} and χ_H become negligible (<1%) once N becomes of the order ~1000. Such a weak N-dependence is expected since the physical origin of χ_{th} and χ_H is spatially *local* enthalpic interactions and interchain packing correlations.

C. Deuteration Swap Effect. Deuteration leads to a decrease in the bond polarizibility density and hence a decrease in the van der Waals interaction of the deuterated chains. Therefore, the Berthelot parameter $\lambda = (\epsilon_{BB}/\epsilon_{AA})^{1/2}$ can increase or decrease depending upon which component of the blend is deuterated. The "swap effect" refers to the experimental observation that deuteration of the more flexible (lower aspect ratio, generally more branched) polyolefin component of the blend leads to an increase in the χ-parameter (i.e., raising of the critical or cloud point temperature T_C) while deuteration of the more stiff component (larger Γ, less branched) decreases the χ-parameter (T_C decreases).[2,3,9,10] This effect appears to be unexpectedly large, and we believe it provides direct experimental evidence for the nonadditivity of the thermodynamic consequences of structural and interaction asymmetries, and the primary role of the (correlated) enthalpic contribution to ΔF_{mix}.

To model this phenomenon, we define λ_D to be the contribution to the Berthelot parameter λ due to the deuteration of a fraction f_D of the protons of one of the blend components. The dependence of λ_D on f_D is given by the simple relation[53]

$$\lambda_D = 1 + x_D f_D \tag{4.1}$$

where the estimate of x_D proposed by various groups[2,3,9,10,54] lies between ~0.006−0.016. In practice, the appropriate value of x_D may also depend on the fraction of deuterated monomers that lie on the backbone versus the side chains. This is because monomers on the backbone may often be partially shielded by their side groups from making significant intermolecular contacts.[30,36,48] Hence, side-chain deuteration may be more effective in changing the χ-parameter than if the same fraction of backbone monomers were deuterated. This physical consideration would lower the effective value of x_D in our simple single site homopolymer model.

If λ characterizes the interaction between the blend components without deuteration, then $\lambda\lambda_D$ and λ/λ_D are the Berthelot parameters upon deuteration of the flexible and stiff components, respectively. The magnitude of the swap effect can then be characterized by a ratio parameter $R = \chi(\lambda\lambda_D)/\chi(\lambda/\lambda_D)$. Exploration and presentation of the behavior of R is a difficult task since R depends on at least four independent variables (Γ_A, Γ_B, λ, λ_D). Therefore, we present results only for what we believe are experimentally relevant[16−18] values of $\Delta\Gamma \leq 0.2$, $\bar{\Gamma} = 0.85-1.35$, and selected λ and λ_D values. In Figures 5a and 5b we plot R as a function of the average aspect ratio $\bar{\Gamma}$ for several blends with different Γ_A and Γ_B (but only $\Delta\Gamma = 0.05$, 0.1, 0.2) and for $\lambda = 1.05$ and $\lambda = 1.024$, respectively, using the full blend theory χ_{th}. Typical values of f_D employed in recent experiments[2,3,9] are $f_D \sim 0.3-0.4$, which implies $\lambda_D \sim 1.002-1.007$. Three representative values of $\lambda_D = 1.002$, 1.004, and 1.008 are chosen to illustrate the dependence of the swap effect on the amount of deuteration. For fixed λ_D, λ, and $\bar{\Gamma}$, there are still variations in the predicted value of R due to the dependence on $\Delta\Gamma$. However, for the cases studied R systematically decreases as $\Delta\Gamma$ increases at fixed $\bar{\Gamma}$, λ, λ_D as expected based on the model calculations of Figures 4.

As λ_D increases the magnitude of swap effect increases (in a statistical sense) as expected since the increased deuteration of the flexible chains weakens their interaction strength and reinforces the structural incompatibility aspect of the components, while the increased deuteration of the stiff chain tends to compensate it. This leads to an enhanced χ-parameter if the flexible component is deuterated while the reverse is true when

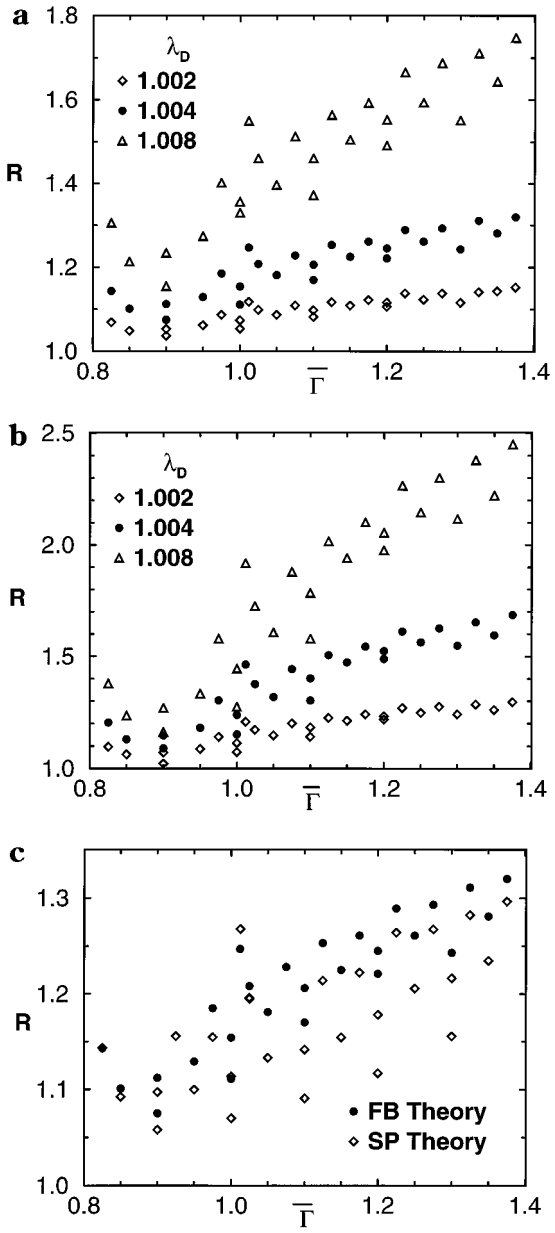

Figure 5. (a) The ratio of the full blend χ-parameter, R, when the flexible chain is deuterated to the χ-parameter when the stiff chain is deuterated as a function of the average aspect ratio $\bar{\Gamma}$ for several model blends with different Γ_A/Γ_B and fixed $\lambda = 1.05$. The values of Γ_A and Γ_B for all of the blends are chosen to be between 0.8 and 1.4 (in increments of 0.05) such that the average aspect ratio falls in the range 0.825 (for $\Gamma_A/\Gamma_B = 0.8/0.85$) and 1.375 (for $\Gamma_A/\Gamma_B = 1.35/1.4$) and $\Delta\Gamma = 0.05-0.2$. Three representative values of $\lambda_D = 1.002$, 1.004, and 1.008 are chosen to illustrate the dependence of the swap effect on the amount of deuteration. (b) Same as Figure 5a but for a smaller value of $\lambda = 1.024$. (c) Comparison of the swap effect χ-parameter ratio, R, as a function of the average aspect ratio $\bar{\Gamma}$ for several blends with different Γ_A/Γ_B and $\Delta\Gamma = 0.05-0.2$ obtained using the full blend theory and the solubility parameter theory. The value of λ is fixed at 1.05 and $\lambda_D = 1.004$.

the stiff chain is deuterated. This qualitative trend and the predicted absolute magnitude of R are in good agreement[37] with the many experimental measurements of the swap effect in polyolefins.[2,3,9]

For all of the cases considered an increase in the average aspect ratio of the blend (which enhances nonrandom mixing $\Delta g(r)$) increases the swap effect in a statistical sense. In Figure 5a this increase is most pronounced for the case where $\lambda_D = 1.008$ since the swap effect is the largest for this case. Again this trend is expected from the behavior documented in Figures 4. Comparison of Figures 5a and 5b also shows that by keeping other parameters fixed, the swap effect is larger in a statistical sense when the chemical interaction asymmetry between the components (denoted by λ) is smaller. This is because the percent change in the interaction asymmetry due to deuteration is larger in this case so that the changes in the χ-parameter due to deuteration are more significant. In principle, these detailed predictions might be experimentally tested, although independent variation of λ_D, λ, Γ_A, and Γ_B is generally not possible. However, the latter can be achieved by carefully designed off-lattice computer simulations. If the interaction asymmetry parameter λ is very large, then the Flory mean field limit is achieved and the deuteration swap effect is negligible. This conclusion also follows for very large conformational asymmetry γ or $\Delta\Gamma$. Both of these limiting cases correspond to when χ is very large and positive.

We have also calculated $R_H = \chi_H(\lambda\lambda_D)/\chi_H(\lambda/\lambda_D)$ using the microscopic solubility parameter theory. The general trends of the predicted R with $\bar{\Gamma}$, $\Delta\Gamma$, λ, and λ_D are analogous to those in the full blend theory for χ_{th}, although the magnitude of the swap effect is typically smaller for χ_H. However, for $\lambda > 1$ the magnitude of swap effect using the two theories agree reasonably well. Some of these conclusions are illustrated in Figure 5c where R for both the solubility parameter and the full blend theories are plotted as a function of $\bar{\Gamma}$ for $\lambda = 1.05$ and $\lambda_D = 1.004$.

A particularly interesting effect is predicted if the system is in the asymmetry compensation parameter regime, i.e., values of $\lambda < 1$ for a given Γ_A/Γ_B where χ_{th} can become negative. The swap effect can then result in a positive or negative value of R depending on the positivity or negativity of both $\chi(\lambda\lambda_D)$ and $\chi(\lambda/\lambda_D)$. For such special values of λ and aspect ratios, $R = \chi(\lambda\lambda_D)/\chi(\lambda/\lambda_D)$ becomes very sensitive to the exact values of the numerator and denominator since both are small. We note that such a $R < 0$ behavior has been observed in a few polyolefin blends which are characterized by very small χ-parameters.[2-4] Although there is no negative χ-parameter in the solubility parameter theory, the trends in the swap effect for $\lambda < 1$ close to maximum miscibility region (minimum χ_H) become erratic due to the sensitivity of the results to the exact values of $\chi_H(\lambda\lambda_D)$ and $\chi_H(\lambda/\lambda_D)$ both of which are very small.

D. Temperature Dependence of χ-Parameter. The predicted thermal dependence of the χ-parameter is complicated due to the *nonuniversal* influences of the temperature dependence of the effective site hard core diameter,[32,33] blend density, and statistical segment length $\sigma = (6R_g^2/N)^{1/2}$. The temperature dependence of the site hard core diameter can be estimated using the standard Barker-Henderson theory[55] which relates d to the continuous repulsive branch of the intersite potential as

$$d = \int_0^\infty dr[1 - e^{-\beta v_0(r)}] \tag{4.2}$$

Here we employ the shifted, repulsive Lennard-Jones potential

$$\begin{aligned} v_0(r) &= 4\epsilon[(r_c/r)^{12} - (r_c/r)^6], \qquad r \le r_c \\ &= 0, \qquad\qquad\qquad\qquad r > r_c \end{aligned} \tag{4.3}$$

To calculate the length r_c the depth of the interaction

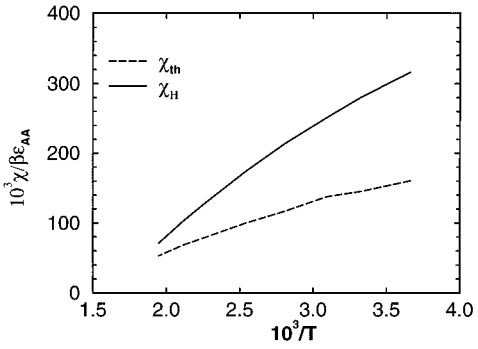

Figure 6. Comparison of the temperature dependence of the reduced χ-parameter obtained using the full blend theory and the solubility parameter theory for $\Gamma_A/\Gamma_B = 1/1.2$ (at $T = T_{ref} = 440$ K) and $\lambda = 1.05$. The temperature range is chosen to be 273 K $\leq T \leq$ 500 K.

potential well is set equal to a typical value for a CH_2 group of $\epsilon = 40$ K, and the hard core diameter is $d(T = 430\ \text{K}) = 3.9$ Å at a reference temperature $T_{ref} = 430$ K. This procedure is identical to prior estimates of $d(T)$ for the RIS model of polyethylene,[56] and yields $r_c = 4.35$ Å. The hard core diameter at a temperature T can then be calculated from the ratio relation

$$\frac{d(T)}{d(T_{ref})} = \frac{\int_0^\infty dr[1 - e^{-\beta_T v_0(r)}]}{\int_0^\infty dr[1 - e^{-\beta_{ref} v_0(r)}]} \tag{4.4}$$

In accord with physical intuition, d (and also the reduced density ρd^3) decreases upon heating. The temperature dependence of the density and effective segment length σ are estimated from the linear relations

$$\rho = \rho_{ref}[1 + \alpha_\rho \Delta T]$$
$$\sigma_M^2 = \sigma_{ref,M}^2[1 + \delta C_M \Delta T] \tag{4.5}$$

where $\Delta T = T - T_{ref}$, α_ρ = thermal expansion coefficient, δC_M = logarithmic derivative of the characteristic ratio C_∞ of polymer M (both α_ρ and δC_M are evaluated at the reference temperature T_{ref}), and ρ_{ref} and $\sigma_{ref,M}$ are the values of ρ and σ_M at a reference temperature.

In Figure 6 we plot the blend χ-parameter in reduced thermal units ($\chi/(\beta\epsilon_{AA})$) as a function of inverse temperature for $\Gamma_A/\Gamma_B = 1.0/1.2$ (at a reference $T = 440$ K) and $\lambda = 1.05$ using both the solubility parameter and the full blend theories over the temperature range 273 K $\leq$ T $\leq$ 500 K. The trivial mean field (T^{-1}) temperature dependence is divided out, so the T-variation seen in Figure 6 is due to the influence of temperature-dependent density and aspect ratios on local blend hard core packing correlations. The above aspect ratios and interaction asymmetry parameters were chosen to crudely mimic a PE−PEE blend,[17] and hence we choose $\delta C_M = -1.2 \times 10^{-3}$/K and 4.0×10^{-4}/K which are values quoted in the literature for PE and PEE, respectively.[8] We note that with the lowering of temperature the effective segment length of PE increases while that of PEE decreases. Hence, the conformational asymmetry is *monotonically enhanced* upon cooling the liquid. The thermal expansion coefficient is chosen to be -8×10^{-4}/K which results in ρd^3 changing by the same factor as in the RIS model for PE ($\rho d^3 = 1.375$ at $T_{ref} = 440$ K).[18]

The aspect ratio at temperature T is evaluated using

$$\Gamma(T) = \Gamma(T_{ref}) \frac{\sigma(T)}{\sigma(T_{ref})} \frac{d(T_{ref})}{d(T)} \tag{4.6}$$

Figure 6 shows that $\chi/(\beta\epsilon_{AA})$ increases monotonically as the temperature decreases. As expected from the model calculations of Figure 4, the primary origin of this trend is the monotonic increase of $\Delta\Gamma = \Gamma_B - \Gamma_A$ from 0.2 at 440 K to ≈ 0.352 at 273 K. However, such a trend is *not* universal. Indeed, a decrease, flat, or even non-monotonic variation of $\chi/(\beta\epsilon_{AA})$ with T^{-1} is possible for different systems depending on the magnitudes and detailed temperature dependences of Γ_A, Γ_B, and ρ. We find $\chi_H > \chi_{th}$ for the case shown, but the two theories agree to within a factor of $\approx$1.4−2 for the parameters chosen. The factor $\beta\epsilon_{AA}$ on a four-carbon basis is $\approx$1.15 at $T = 440$ K (see Section III of ref 18). Hence, the absolute magnitude of the predicted χ_{th} on a four carbon basis varies from $\approx 800 \times 10^{-4}$ at 440 K to $\approx 2500 \times 10^{-4}$ at 300 K. Graessley et al.[2,7] have estimated the χ-parameter for PE−PEE blend at various temperatures based upon the knowledge of the experimentally-deduced solubility parameters using eq 3.9 (note that PE/PEE blends are immiscible). The result is:[2,7] $10^4\chi \sim 950-450$ for $T = 27-167$ °C (on a four-carbon basis) which is within a factor of 2−3 of the theoretical predictions of Figure 6. Since we have made no attempt to precisely model PE/PEE blends by judiciously choosing Γ_A, Γ_B, λ, etc., such agreement should be viewed as a plausibility check on the theory which we find highly encouraging.

Figure 6 also suggests that only over a limited temperature window can the χ-parameter be rigorously fitted to the common empirical form $\chi_{eff} = A + B/T$, where in general A and B can have either sign within our theory. LCT studies of polyolefins have come to a similar conclusion.[31] We emphasize that our predicted $\chi(T)$ does correspond to nonzero A and B factors, the precise values of which are influenced by monomer structure and (indirectly) the effect of $\rho(T)$, $\sigma(T)$, $d(T)$, etc. We emphasize that the physical origin of $A \neq 0$ is *not* pure excess "entropic" or "athermal" effects. Since *only* correlated enthalpic effects enter our calculation, the empirical interpretation of A and B as "entropic" and "enthalpic" is misleading.

Model calculations for blends with other chain-aspect ratios show that the apparent values of A and B over a given temperature range are strongly dependent on the chain microstructure (Γ_A, Γ_B, λ) and also quite sensitive to the thermal and coil expansion coefficients.[37] Broadly speaking, such behavior is again consistent with experimental observations.[2−10]

Finally, at a fixed temperature, $\chi/(\beta\epsilon_{AA})$ increases with increase in λ for the $\Gamma_A/\Gamma_B = 1/1.2$ blend. For example, $10^3\chi_{th}/(\beta\epsilon_{AA})$ at $T = 356$ K are 17.40, 116.71, and 239.15 for $\lambda = 1$, 1.05, and 1.1, respectively, and $\chi_H/(\beta\epsilon_{AA}) =$ 128.31, 213.83, and 321.08 using the Hildebrand-like theory; at $T = 440$ K, $\chi_{th}/(\beta\epsilon_{AA}) = 14.12$, 79.72, and 167.33, and $\chi_H/(\beta\epsilon_{AA}) = 70.53$, 129.11, and 205.28.

E. Masterplot Based on Thread Model Scaling. In ref 18 we derived an analytical expression for χ_H in terms of the conformational and interaction asymmetries between the components based upon a fully flexible Gaussian *thread level* solubility parameter description and PRISM theory:

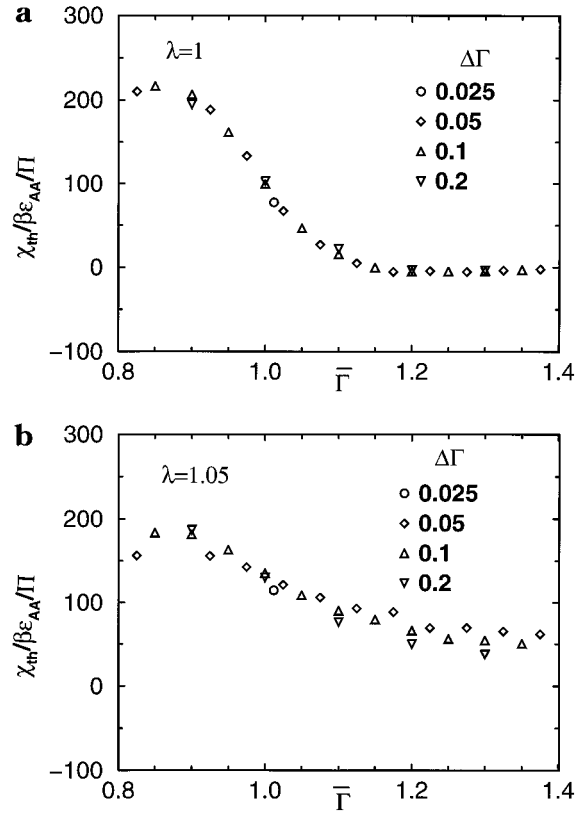

Figure 7. (a) Masterplot obtained by scaling the numerically computed full blend χ-parameter by the analytic thread model based factor, Π, given in eq 4.7. The values of Γ_A and Γ_B for various blends fall in the range 0.8 and 1.4, and $\lambda = 1$. (b) Same as Figure 7a but for $\lambda = 1.05$.

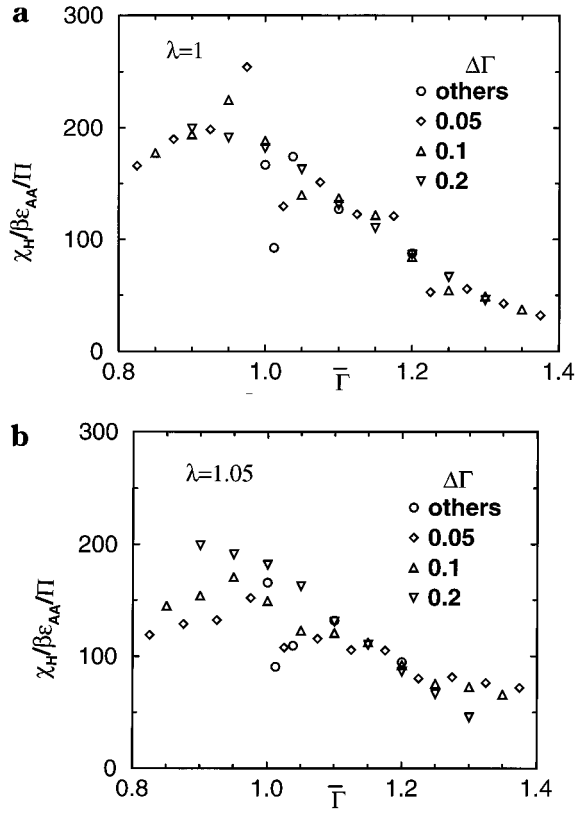

Figure 8. (a) Same as Figure 7a but for the numerical solubility parameter theory where $\chi = \chi_H$. (b) Same as Figure 7b but for the numerical solubility parameter theory.

$$\chi_H = 6\beta\eta\Delta^3\epsilon_{AA}\Pi$$

$$\Pi = \lambda\left[\frac{\lambda^{1/2}}{\sqrt{1+\frac{1}{\Delta 2\eta\Gamma_B^2}}} - \frac{\lambda^{-1/2}}{\sqrt{1+\frac{1}{\Delta 2\eta\Gamma_A^2}}}\right]^2 \quad (4.7)$$

where $\eta = \pi\rho d^3/6$, $\Delta = a/d$, a is the range of the interaction potential assumed to be of the Yukawa form for analytical convenience within the thread formalism ($v(r) = -\epsilon(a/r)\exp(-r/a)$),[11] and Γ_A and Γ_B are the aspect ratios of the two blend components, $\Gamma_M = \sigma_M/d$. The predictions of this analytic thread model χ-parameter[18] were found to be qualitatively consistent (and in some cases in semiquantitative agreement) with many non-mean field observations for polyolefin blends. Here we empirically test whether a similar dependence on molecular parameters as in eq 4.7 might (approximately) hold for the χ-parameters obtained numerically for semiflexible, finite d chains at the full blend and solubility parameter levels.

The ratio χ/Π is plotted versus $\bar{\Gamma} = (\Gamma_A + \Gamma_B)/2$ in Figures 7 and 8 for the full blend and solubility parameter theories, respectively. If eq 4.7 exactly described the numerical results, then a complete collapse to a single number for all choices of Γ_A, Γ_B, and λ would occur. We note that the attractive tail potential in the numerical calculations is chosen to be of the shifted Lennard−Jones form given in eq 2.2 rather than the Yukawa form with an interaction range "a" as was done in the thread calculations. Because of this difference, the value of Δ in eq 4.7 is adjusted to obtain the best collapse of the curves for blends characterized by different values of Γ_A, Γ_B, and λ. If $\eta = 0.5$, then for all the cases considered $\Delta = 0.5$ gave the best collapse; this is reassuring since earlier mappings of the Lennard−Jones onto the Yukawa potential suggest that $\Delta \approx 0.5$ is the value of potential which best mimics the LJ 6−12 interaction.[21] Figures 7a and 7b show that for a fixed value of λ and $\bar{\Gamma}$, χ_{th}/Π using the full blend theory collapses to a reasonable extent for all $\Delta\Gamma = \Gamma_B - \Gamma_A$, although the value of χ_{th}/Π is not constant for all $\bar{\Gamma}$. In particular, for all the λ values χ_{th}/Π initially decreases between $\bar{\Gamma} = 0.8$ and 1.1 and then becomes nearly constant. The plot of χ_{th}/Π vs $\bar{\Gamma}$ for different λ collapses quite well for the cases where χ_{th} is positive, but not in the region where the χ-parameter becomes negative for a given λ and the structural and interaction asymmetries compete with each other (e.g., compare high $\bar{\Gamma}$ region for $\lambda = 1$ with $\lambda = 1.05$). This is expected since the thread-solubility parameter theory which yields eq 4.7 is incapable of accounting for negative χ-parameters in the compensation region.

Figures 8 are analogous to Figures 7 but using the numerical solubility parameter theory. In this case we find a reasonable collapse of χ_H/Π for a fixed $\bar{\Gamma}$ for all λ (including $\lambda = 1.02$ not shown), but χ_H/Π typically decreases with increase in $\bar{\Gamma}$. Curiously, the scatter in the collapsed data appears to be more for the solubility parameter theory than the full blend theory.

V. Model Calculations: Random Copolymer Blends

A binary random copolymer consists of a fraction x of one type of monomer (reference polymer 1) randomly distributed along the chain with fraction $(1-x)$ of another type of monomer (reference polymer 2). We consider a binary blend of random copolymers where for simplicity both components of the random copolymer

Table 2. Model Calculations Showing the Typical Magnitudes Predicted for the Swap Effect in Random Copolymer Blends Characterized by $R = \chi(\lambda_{eff}\lambda_D)/\chi(\lambda_{eff}/\lambda_D)$ for $\Gamma_{ref,1} = 1.0$ and $\Gamma_{ref,2} = 1.2$ Using $\chi = \chi_{th}$ of the Full Blend Theory[a]

	$\lambda = 1.1$			$\lambda = 1.05$			$\lambda = 0.95$		
	λ_D			λ_D			λ_D		
Y_A/Y_B	1.002	1.004	1.008	1.002	1.004	1.008	1.002	1.004	1.008
97/88	1.49	2.27	6.41	1.92	4.18	(−20.92)	(−0.02)	(−0.42)	(−0.85)
88/78	1.47	2.20	5.92	1.86	3.79	(−38.0)	(0.13)	(−0.27)	(0.72)
78/66	1.42	2.05	4.79	1.81	3.53	(−110.0)	(0.39)	(0.03)	(−0.44)
66/52	1.41	2.01	4.58	1.76	3.37	181.0	(0.53)	(0.23)	(−0.21)
52/38	1.44	2.13	5.23	1.88	3.89	(−35.0)	(0.60)	(0.30)	(−0.14)
38/25	1.53	2.37	7.11	2.22	6.04	(−10.0)	(0.64)	(0.36)	(−0.11)
35/17	1.35	1.84	3.62	1.71	3.07	28.77	(0.71)	(0.49)	(0.11)
32/0	1.19	1.42	2.05	1.39	1.95	4.23	(0.86)	(0.73)	(0.51)
25/8	1.39	1.96	4.16	1.86	3.79	(−61.6)	(0.74)	(0.52)	(0.14)
25/0	1.26	1.59	2.60	1.51	2.35	7.28	(0.82)	(0.66)	(0.38)
17/0	1.40	1.98	4.27	1.89	3.90	(−48.3)	(0.76)	(0.55)	(0.15)

[a] The calculations are performed for reference system chemical asymmetry parameters of 1.1, 1.05, and 0.95, and $\lambda_D = 1.002$, 1.004, and 1.008 for each λ. The R values in brackets refer to the cases where at least one of the χ-parameters is negative. λ_{eff} is given by eq 5.2. The Y_A/Y_B choices correspond to cases studied experimentally for *PE/PEE* systems.[2,3,9,10]

blend consists of the same types of monomers. Therefore, the two components of the random copolymer blend differ only in the relative proportion in which the two monomers are distributed in the two random copolymer components. For example, a Y_A/Y_B random copolymer blend of polyethylene (PE-unbranched) and polyethylethylene (PEE-branched) is a blend in which random copolymer A has Y_A fraction of PEE. (and hence $(1 - Y_A)$ fraction of PE) while the B component has Y_B fraction of PEE.

From a statistical mechanics perspective, quenched sequence randomness introduces additional theoretical difficulties. Here, we consider the simplest possible approach:[20] preaverage the quenched inhomogeneities to obtain an effective homopolymer description. Although the accuracy of such a simplification is apriori unknown, recent polyolefin experiments have found examples where the effective χ-parameter is not sensitive to whether the copolymer is random or strictly alternating.[2,5] In addition, there is the hope that the irregular space filling nature of random copolymers makes the use of coarse-grained, effective monomer models more appropriate.

We have studied two homologous series of random copolymer blends with the aspect ratios of the two reference polymers $\Gamma_{Ref,1}/\Gamma_{Ref,2} = 1.0/1.2$ and 1.1/1.2, which roughly mimics PEE/PE and PEP/PE, respectively.[17,18,46] The aspect ratio Γ_M for the random copolymer M is obtained by a Gaussian interpolation formula

$$\Gamma_M^2 = Y_M\Gamma_{Ref,1}^2 + (1 - Y_M)\Gamma_{Ref,2}^2 \tag{5.1}$$

where Y_M is the fraction of the reference polymer 1 with aspect ratio $\Gamma_{Ref,1}$. This simple relation has been shown by Bates et al.[57] to be remarkably accurate for describing the statistical segment lengths of random polyolefin copolymers. If λ is the Berthelot parameter associated with the reference homopolymers, then the λ_{eff} for the random copolymer blend is given by a simple preaveraging relation:[20]

$$\lambda_{eff} = \frac{Y_B + (1 - Y_B)\lambda}{Y_A + (1 - Y_A)\lambda} \tag{5.2}$$

A. Copolymer Compositional Effects and Failure of Mean Field Theory. According to the classical incompressible mean field theory (Flory−Huggins) of random copolymer blends[58] the dependence of the effective χ-parameter on random copolymer composition is exclusively through the square of the compositional difference:

$$\chi_{FH} = (Y_B - Y_A)^2\chi_B^0 \equiv (\Delta Y)^2\chi_B^0 \tag{5.3}$$

where χ_B^0 is the Flory−Huggins χ-parameter of the homopolymer blend composed of the reference polymers. For the shifted Lennard−Jones tail potential of eq 2.2, χ_B^0 is given by

$$\chi_B^0 = 10\pi\beta|\epsilon_{AA}|\rho d^3(\lambda - 1)^2/9 \tag{5.4}$$

Experimentally, the χ-parameter of blends of random polyolefin copolymers[2,3,5,9,10] have been found to depend not only on the compositional difference of the components, $\Delta Y = Y_B - Y_A$, but also on the average composition $\bar{Y} = (Y_A + Y_B)/2$. Within the microscopic solubility parameter formalism[18] the random copolymer effect can be understood in terms of the dependence of the difference in the solubility parameters on $\bar{\Gamma}$ even if $\Delta\Gamma$ is the same. Experimentally, for the polyolefin random copolymer blends as the average branch content increases (i.e., the chains become more flexible on average), the quantity $\chi/(\Delta Y)^2$ increases.[2,5,9] Prior analytic thread solubility parameter theory[18] and our present numerical model calculations both show that the dependence of $\chi/(\Delta Y)^2$ on $\bar{Y}$ is a nonuniversal function of λ and the aspect ratios of the components, and it can increase, decrease, or even show a non-monotonic dependence on $\bar{Y}$. For parameters relevant for polyolefins, however, there is generally an increase with mean branch content similar to those seen in the experiments.[2,5,9]

In Figures 9 we plot $\tilde{\chi}/(\Delta Y)^2$ vs $\bar{Y}$ (where $\tilde{\chi} = \chi/(\beta\epsilon_{AA})$) for several values of λ (spanning the range of typical real system possibilities) using both the microscopic solubility parameter and the full blend theories. The aspect ratio choice of $\Gamma_{Ref,1}/\Gamma_{Ref,2} = 1.0/1.2$ roughly mimics PEE/PE. The Y_A/Y_B values chosen were motivated by experimental studies of PE/PEE random copolymer blends[2,5,9] and are listed in Tables 2 and 3. Figure 9a shows that for $\lambda = 1.05$ and 1.1 (corresponding to the asymmetry reinforcement regime), $\bar{\chi}/(\Delta Y)^2$ increases monotonically as a function of $\bar{Y}$. The rate of increase of $\bar{\chi}/(\Delta Y)^2$ is relatively slow for smaller $\bar{Y}$, especially when the full blend theory is used where mean field behavior is quite well followed up to $\bar{Y} \approx 0.5$. The absolute magnitude of χ-parameters using both the solubility parameter and the full blend theories agree

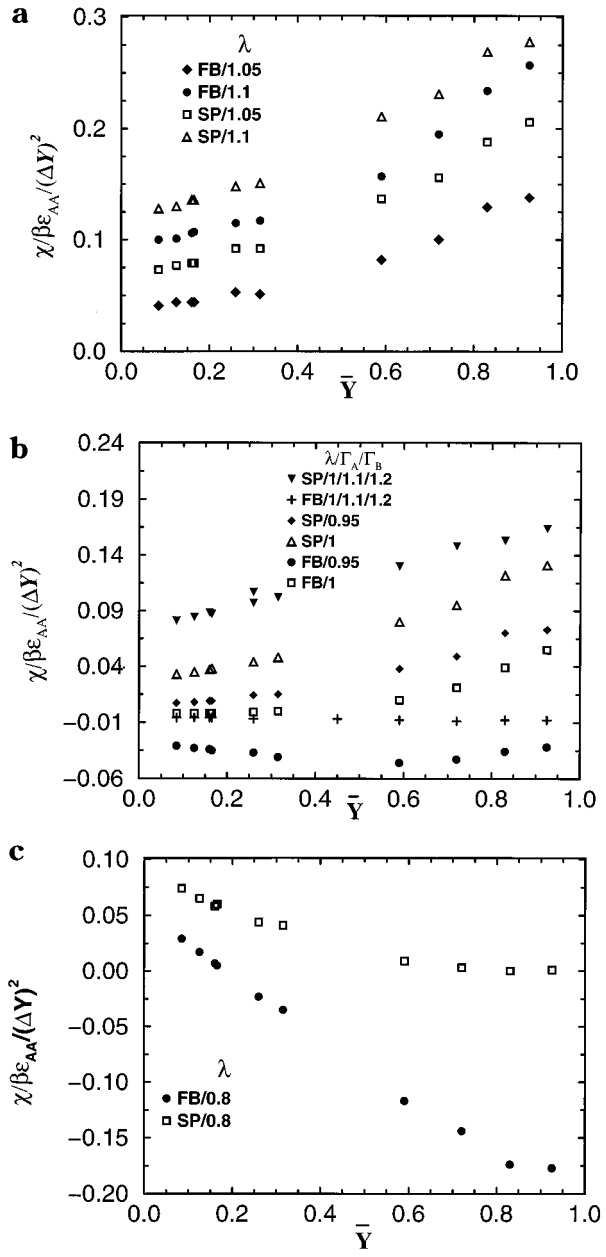

Figure 9. (a) Blend χ-parameter scaled by the compositional difference, ΔY, $(\chi/(\beta\epsilon_{AA})/(\Delta Y)^2)$ versus the average blend composition using both the full blend (FB) theory and the solubility parameter (SP) theory for $\Gamma_{Ref,1}/\Gamma_{Ref,2} = 1/1.2$. The chemical asymmetry parameters are $\lambda = 1.1$ and 1.05. (b) Blend χ-parameter scaled by the compositional difference, ΔY, $(\chi/(\beta\epsilon_{AA})/(\Delta Y)^2)$ versus the average blend composition using both the full blend (FB) theory and the solubility parameter (SP) theory for $\Gamma_{Ref,1}/\Gamma_{Ref,2} = 1/1.2$ and 1.1/1.2. The chemical asymmetry parameters are $\lambda = 1$ and 0.95 for $\Gamma_{Ref,1}/\Gamma_{Ref,2} = 1/1.2$, and $\lambda = 1$ for $\Gamma_{Ref,1}/\Gamma_{Ref,2} = 1.1/1.2$. The legends that do not show the values of $\Gamma_{Ref,1}/\Gamma_{Ref,2}$ correspond to 1/1.2. (c) Blend χ-parameter scaled by the compositional difference, ΔY, $(\chi/(\beta\epsilon_{AA})/(\Delta Y)^2)$ versus the average blend composition using both the full blend (FB) theory and the solubility parameter (SP) theory for $\Gamma_{Ref,1}/\Gamma_{Ref,2} = 1/1.2$. The chemical asymmetry parameter is $\lambda = 0.8$.

quite well. Based on the full blend theory, the overall increase of $\chi/(\Delta Y)^2$ is by a factor of $\approx$2.5 for $\lambda = 1.1$ and a factor $\approx$4 for $\lambda = 1.05$. The corresponding increases using the solubility parameter theory are by factors of $\approx$2.3 and 2.7. The trends and magnitude of deviations from mean field theory agree well[37] with experiments on PE/PEE blends[2,3,5,9] as previously documented using the thread analytic solubility parameter theory.[18] Figure 9b shows predictions for two choices of aspect ratios. For $\lambda = 1$ and $\Gamma_{Ref,1}/\Gamma_{Ref,2} = 1.0/1.2$, $\tilde{\chi}(\Delta Y)^2$ has a trend similar to that of $\lambda = 1.1$ in Figure 9a, but it increases by a larger amount as a function of $\bar{Y}$. For example, for the full blend theory, $\chi/(\Delta Y)^2$ increases from a slightly negative value to 0.056 while the corresponding change using the solubility parameter theory is from $\sim$0.032 to $\sim$0.132.

Figure 9b also plots results for $\lambda = 0.95$ (in the asymmetry compensation regime) and shows that $\tilde{\chi}(\Delta Y)^2$ using the full blend theory has a non-monotonic trend with $\bar{Y}$ and remains negative for the whole range of copolymer compositions. The solubility parameter theory for $\lambda = 0.95$ on the other hand shows a monotonic increase from $\chi/(\Delta Y)^2 = 0.006$ to 0.074 over the whole range. Figure 9c shows that for $\lambda = 0.8$, $\tilde{\chi}(\Delta Y)^2$ using the full blend theory undergoes a sign change and shows a monotonic decrease with $\bar{Y}$ going from 0.3 to -0.18. The trend in $\bar{\chi}(\Delta Y)^2$ with $\bar{Y}$ for $\lambda = 0.8$ using the solubility parameter theory is also a monotonic decrease from 0.075 to 0.0.

Examples of the predicted trends of $\tilde{\chi}(\Delta Y)^2$ for the choice $\Gamma_{Ref,1}/\Gamma_{Ref,2} = 1.1/1.2$ (crudely mimics PEP/PE) and various λ are given in Figure 9b. The results are similar to that for $\Gamma_{Ref,1}/\Gamma_{Ref,2} = 1.0/1.2$ except that the relative changes with $\bar{Y}$ are larger for the latter, more conformationally asymmetric case as expected. To illustrate this we have plotted $\chi/(\Delta Y)^2$ for $\Gamma_{Ref,1}/\Gamma_{Ref,2} = 1.1/1.2$ and $\lambda = 1$ along with $\Gamma_{Ref,1}/\Gamma_{Ref,2} = 1.0/1.2$ in Figure 9b. To the best of our knowledge no experimental data exists for PEP/PE random copolymer blends. Finally, in the extreme limits $\lambda \gg 1$ or $\Delta\Gamma \rightarrow 0$ the mean field Flory theory of eq 5.3 is recovered.

B. Deuteration Swap Effect. There have been a large number of deuteration swap effect experiments performed on blends of random copolymer olefins, particularly for PE/PEE, and empirical solubility parameter arguments have been advanced to explain them.[2,3,9,10] These measurements motivate the calculations of this section which employ aspect ratios relevant to PE, PEP, and PEE, and values of λ which span the plausible possibilities.[17,18] Results for the ratio $R = \chi(\lambda_{eff}\lambda_D)/\chi(\lambda_{eff}/\lambda_D)$ are listed in Tables 2−4 for various random copolymers with the fraction of polymer with an aspect ratio $\Gamma_{Ref,1}$ in the two components being denoted by Y_A and Y_B as shown in column 1. As in section A above, the selected values of Y_A/Y_B are motivated by recent *PE/PEE* random copolymer blend experiments.[2,3,9]

Tables 2 and 3 show the swap effect predictions using the full blend theory and the solubility parameter theory, respectively, for $\Gamma_{Ref,1}/\Gamma_{Ref,2} = 1.0/1.2$, three different Berthelot parameters $\lambda = 1.1$, 1.05, and 0.95, and for three levels of deuteration $\lambda_D = 1.002$, 1.004, and 1.008. The λ_{eff} for each random copolymer blend with a fixed λ and Y_A/Y_B is determined by using eq 5.2. One obvious feature that emerges from comparing Figures 5a and 5b with results in Tables 2 and 3 is that the swap effect is much larger for random copolymer blends than for the homopolymer blends made with the reference polymers. This is not surprising because the interaction asymmetry between the components of the random copolymer blend is relatively small (i.e., λ_{eff} for the random copolymer blends is close to *one* even for $\lambda = 1.1$, 1.05, and 0.95). Also, the structural asymmetry between the components of the homopolymer blends is larger than the random copolymer blends made with the same monomers. In the presence of such small intrinsic interaction and structural asymmetry the

Table 3. Same as Table 2 but Based on the Numerical Solubility Parameter Approach Where $\chi = \chi_H$

	$\lambda = 1.1$			$\lambda = 1.05$			$\lambda = 0.95$		
	λ_D			λ_D			λ_D		
Y_A/Y_B	1.002	1.004	1.008	1.002	1.004	1.008	1.002	1.004	1.008
97/88	1.32	1.75	3.14	1.38	1.92	3.83	1.73	3.07	11.53
88/78	1.30	1.69	2.91	1.37	1.57	3.62	1.67	2.83	9.43
78/66	1.27	1.62	2.65	1.34	1.80	3.32	1.68	2.88	9.87
66/52	1.25	1.55	2.44	1.31	1.73	3.05	1.69	2.89	9.93
52/38	1.28	1.64	2.73	1.35	1.83	3.47	1.90	3.74	20.42
38/25	1.34	1.79	3.30	1.45	2.12	4.73	2.57	7.48	922.0
35/17	1.24	1.53	2.38	1.31	1.72	3.04	2.02	4.24	30.25
25/8	1.27	1.61	2.63	1.36	1.87	3.62	2.55	7.27	484.0
32/0	1.14	1.29	1.67	1.18	1.40	1.96	1.66	2.80	9.18
25/0	1.18	1.40	1.96	1.24	1.54	2.41	1.96	3.99	24.70
17/0	1.28	1.64	2.74	1.39	1.94	3.90	3.03	11.17	835.0

Table 4. Same as Tables 2 and 3 for Values of $\Gamma_{ref,1} = 1.1$ and $\Gamma_{ref,2} = 1.2$ Roughly Characteristic of PEP/PE Random Copolymers

	solubility parameter						full blend					
	$\lambda = 1.1$ λ_D			$\lambda = 1.05$ λ_D			$\lambda = 1.1$ λ_D			$\lambda = 1.05$ λ_D		
Y_A/Y_B	1.002	1.004	1.008	1.002	1.004	1.008	1.002	1.004	1.008	1.002	1.004	1.008
97/88	1.68	2.88	9.86	2.02	4.28	31.42	1.83	3.51	30.30	2.79	12.17	(−10.25)
88/78	1.61	2.62	7.79	1.97	4.40	25.82	1.74	3.16	17.50	2.85	15.40	(−17)
78/66	1.49	2.24	5.39	1.77	3.21	13.08	1.59	2.59	8.21	2.28	6.53	(−14.18)
66/52	1.42	2.03	4.34	1.66	2.82	9.32	1.50	2.28	5.96	2.09	4.87	(−25.71)
52/38	1.47	2.17	5.00	1.71	3.00	10.94	1.55	2.47	7.26	2.13	5.12	(−23.7)
38/25	1.52	2.34	5.95	1.85	3.53	17.02	1.61	2.68	9.26	2.44	7.42	(−14.5)
35/17	1.35	1.84	3.47	1.54	2.40	6.34	1.41	2.01	4.32	1.81	3.44	37.83
32/0	1.19	1.42	2.02	1.29	1.68	2.87	1.22	1.48	2.23	1.43	2.06	4.73
25/8	1.39	1.93	3.88	1.63	2.69	8.30	1.45	2.12	4.91	1.96	4.16	(−196.0)
25/0	1.25	1.58	2.51	1.39	1.94	3.93	1.29	1.68	2.89	1.57	2.52	8.10
17/0	1.39	1.95	3.95	1.64	2.74	8.71	1.45	2.13	4.97	2.00	4.20	(−192.0)

change in the χ-parameter due to deuteration makes a much more significant difference.

The results in Table 2 show no obvious pattern of the change in the swap effect with increase in $\bar{Y}$ (e.g., for PE/PEE as the average branch content increases). For example, for $Y_A/Y_B = 32/0$ the swap effect is the smallest while for $Y_A/Y_B = 38/25$ it is largest. Similar features have been found in the experiments on random copolymer blends of *PE/PEE*.[3] We attribute these features to the non-monotonic dependence of λ_{eff} given in eq 5.2 on $\bar{Y} = (Y_A + Y_B)/2$ for various values of Y_A/Y_B. For example, for a blend with $Y_A/Y_B = 32/0$, λ_{eff} is largest of all the random polymer blends while it is smallest for a blend with $Y_A/Y_B = 38/25$. Similar to the homopolymer case, an increase in λ_D for a fixed λ increases the deuteration swap effect, and an increase in λ for a fixed λ_D decreases it. For small values of λ, the χ-parameter and the ratio R computed from the full blend theory can be negative. All the cases which involve one or both negative χ-parameters are shown in the tables in parentheses. We note that for cases where both the χ-parameters are negative, R is positive. Experiments on a few random polyolefin blends have shown a negative R.[4] Comparison of Table 2 and Table 3 also shows that the solubility parameter theory predicts a smaller swap effect than that predicted by the full blend theory for the same parameters. Moreover, since $\chi_H > 0$ always, R is never negative. The general trends in the swap effect as a function of λ, λ_D and the composition of the random copolymer blend Y_A/Y_B using the solubility parameter theory is similar to the full-blend theory.

In Table 4, R is tabulated for $\Gamma_{Ref,1}/\Gamma_{Ref,2} = 1.1/1.2$ (crudely representative of the PEP/PE case), and $\lambda = 1.1$ and 1.05, based on both χ_H and χ_{th} for several random copolymers with the same Y_A/Y_B as in Table 2 and Table 3. The purpose of these calculations is to assess the effect of Γ_{Ref} on the swap effect. We find that the swap effect is somewhat larger than the corresponding results in Tables 2 and 3. This implies that a decrease in $\Delta\Gamma_{Ref}$ enhances the swap effect. This is expected since a weaker structural asymmetry between the blend components will exaggerate the incompatibility effects due to small changes in the interaction asymmetry induced by deuteration. The general trends in the relative magnitude of swap effect as a function of λ, λ_D, and the composition of the random copolymer blend Y_A/Y_B in Table 4 are similar to those in Tables 2 and 3. Finally, as noted earlier, if the inherent interaction asymmetry parameter is $\lambda \gg 1$ or $\Delta\Gamma \gg 1$, no significant swap effect is found, i.e., $R \rightarrow 1$.

VI. Summary and Conclusions

Definitive determination of the primary microscopic physical origin(s) of non-mean-field corrections to the excess free energy of mixing of polymer alloys is a very difficult task from experimental, theoretical, or computer simulation viewpoints. It is often difficult to even establish whether failure of a theory to agree with a particular experimental observation is due to limitations of the statistical mechanical approximations, oversimplification of the molecular model, or both. In principle, computer simulations can clearly separate these issues, but the very large computational effort to investigate off-lattice molecular models relevant to real high polymer alloys is only just beginning to emerge.

In this paper we have numerically investigated the thermodynamics of mixing behavior of conformationally and energetically asymmetric model binary blends using off-lattice compressible PRISM theory for determining the athermal interchain pair correlations, a thermodynamic perturbation approach for computing the enthalpic blend free energy, and an intermediate-level semi-

flexible chain model. Within a liquid state theory context, we view both our model and statistical mechanical approach as a minimalist one which retains the bare essentials of molecular structure, assumes constant volume, ignores conformational nonideality effects, and focuses solely on the correlated enthalpic contribution to the miscibility question. Even given these simplifications, our systematic model calculations with parameters representative of real hydrocarbon materials reveal an extremely rich and subtle mixing behavior which appears to semiquantitatively account for a host of non-mean-field behaviors recently observed for polyolefin blends.[2−10] Three broad regimes are found depending on whether the nonadditive thermodynamic consequences of conformational and energetic (or chemical) asymmetries strongly reinforce ($\gamma > 1$, $\lambda > 1$), strongly compensate ($\gamma > 1$, $\lambda < 1$), or are in a crossover regime ($\gamma > 1$, $\lambda \approx 1$).

Most polyolefins are in the asymmetry reinforcement regime since simple branching in homopolymers increases the methyl group content and reduces both the effective chain aspect ratio (which controls interchain packing efficiency) and interchain dispersion attraction.[17,18] An immediate consequence is that relatively large positive χ-parameters are predicted. Nevertheless, many non-mean-field behaviors are also predicted which are broadly consistent with experiment. These include failure of group additivity schemes, a strong deuteration swap effect, failure of the mean field random copolymer theory, and the possibility of unusual temperature dependences of χ including an apparent "entropic" contribution of correlated enthalpic origin. The latter effect arises from the implicit temperature dependences of conformational properties and density which modify local interchain packing and hence the blend enthalpy. Heating-induced lower critical solution temperature (LCST) type behavior can also emerge for special situations. However, the asymmetry reinforcement regime is also simple in several respects. The effective χ-parameter is nearly N and blend composition independent. Remarkable qualitative, and sometimes nearly quantitative, consistency of the blend theory predictions for the thermal χ-parameter with a microscopic solubility parameter approach based on pure component structure has been demonstrated. An intriguing consistency of χ_{th} with an empirical estimate of a χ-parameter from the heat of mixing has also been found.

A particularly novel prediction of our theory is the possibility that strong asymmetry compensation can result in a negative χ_{th} even in the absence of any "specific energetic interaction". The mathematical origin of this effect is the nonuniversal blend composition dependence of the local packing correlations. For olefin type polymers, practical realization of the required molecular parameter relationships are unlikely, consistent with there being only a very few reports of negative χ-parameters in polyolefins.[2,4,50] However, the theory does make suggestions for rational chemical or physical design strategies for possibly achieving the required conditions. These include clever monomer choices to achieve the $\gamma > 1$, $\lambda < 1$ condition. A particularly promising strategy is to synthesize binary or ternary random copolymers[57] where the chain branch content is "tuned" to control the conformational and bare energetic properties such that the better packing (higher aspect ratio) polymer is the more weakly interacting species in a van der Waals potential sense. Another strategy involves the use of selective deuteration where both the level, and which species is deuterated, are controlled. Indeed, strong swap effects are predicted for many blends (especially random copolymer alloys), including the possibility that the sign of the χ-parameter can change by swapping the deuteration species. These predictions are in good semiquantitative accord with polyolefin experiments.[2−7,9,10] The Hildebrand or microscopic solubility parameter approach cannot predict negative χ-parameters and hence it makes significant errors in the asymmetry compensation parameter range. However, even here some qualitative features remain quite similar to the full blend theory predictions in several broader respects.

From a more general perspective, an advantage of our present approach is that only a relatively few molecular parameters enter the minimalist model. These parameters have a well defined structural meaning and can often be a priori estimated based on known conformational and chemical information.[17,18,37,46] Thus, we hope our model calculations can be employed to both interpret the large existing data base on polyolefins (and possibly polydienes) and also to make testable predictions for yet-to-be studied systems. The use of the theory to make experimentally relevant predictions would be significantly enhanced if there were more high accuracy direct measurements of chain conformational properties as a function of temperature and monomer structure, including random copolymer systems. Direct confrontation of the present theory with experimental small angle neutron scattering and cloud point data on of order 100 binary polyolefin blends will be presented in a future publication.[37]

An equally important future direction is the design and execution of new simulations of polymer blends which can unambiguously test our novel statistical mechanical predictions for the *same* coarse-grained chain models used by the theory. This process has been recently initiated by Kumar and Weinhold[27,29] based on off-lattice Monte Carlo methods. Verification of a basic PRISM prediction[20] of the destabilizing effect of conformational asymmetry in thermal blends even if the bare Flory χ-parameter is zero has been demonstrated,[29] but much more work of this kind is desirable.

Finally, it is worth briefly enumerating all the limitations and simplifications of the present theory and model which deserve attention in future theoretical studies. The simplifications are of two fundamentally different natures: statistical mechanical approximations and molecular model oversimplifications, although their consequences may be coupled. The statistical mechanics issues include the following. (i) Relaxation of the constant volume assumption to access the consequences on miscibility of a blend composition dependence of the liquid density, volume of mixing changes, and high pressure effects. (ii) The influence of the "athermal", or "excess entropic", part of the χ-parameter may not always be very small. PRISM theory as it now exists is able to address this question.[13,18,27,36,51] (iii) For random copolymers the consequences of quenched disorder are unknown. Treatment at the simple level of employing quenched averaged intramolecular structure factors is possible and represents an interesting first step. (iv) Higher order statistical mechanical effects such as (temperature and composition dependent) changes in single chain conformation upon going from the pure one-component melt to a blend, and thermally induced local packing changes (e.g., preferential clustering), could be important for some systems. Both of these

effects can be treated at the expense of more numerical effort based on the "self-consistent" formulation of PRISM,[15,59−64] and the "molecular closure" approximation schemes[15,20,22,25,46] or liquid state "optimized random phase approximation"[65] methods, respectively. (v) The issue of consistency of thermodynamic predictions derived from the compressibility route (CR) versus the free energy route (FR) is also a concern[15,32,33] Prior PRISM compressibility route work for conformationally and interaction asymmetric blends[20,46] is broadly consistent with the predictions of the present paper based on the free energy route. However, one expects there are always some questions which could be at least quantitatively sensitive to this inherent limitation of essentially all integral equation methods[32,33] For example, there are some differences in the detailed prediction of how conformational and energetic asymmetries compete between the CR[20,46] and the present FR approach. Also, the prediction of a negative χ-parameter does not appear to naturally emerge at the CR level previously studied using molecular closure schemes.[20] Again, simulation could play the key role in resolving these often subtle issues.

With regards to limitations of the molecular models, there are also several distinct issues. (i) The influence on packing and thermodynamic properties of molecular features such as different repeat unit volumes, monomer shape, and explicit side-chain branching and symmetry inequivalent sites is a subtle question recently studied using both LCT,[31] and PRISM theory via the free energy/HTA route by Curro and co-workers.[28,30,36,51] By comparing the predictions of such atomistic PRISM models with those of more coarse-grained descriptions, one can gain some knowledge of the role of detailed structural features. The small amount of PRISM work done in this direction is encouraging with regards to the usefulness of properly constructed intermediate level coarse grained models.[17,37] However, the generality and quantitative reliability of this conclusion is unknown. (ii) Corrections to the minimalist Berthelot model of the interchain attractive dispersion forces are largely unknown, although straightforwardly addressable within numerical or analytical PRISM theory.[20] For some systems big consequences could emerge, an obvious example being a true specific interaction blend where stabilizing hydrogen bonding or charge transfer interactions between unlike monomers are present.

Although all the above limitations deserve serious consideration, it seems most useful to first try to determine how far one can get in understanding the complex and rich miscibility behavior of hydrocarbon alloys with a simpler model and theory such as presented in this paper. This effort will be the subject of our next paper in this fascinating area of polymer science and engineering.

Acknowledgment. We thank W. Graessley, R. Krishnamoorti, E. David, J. G. Curro, J. J. Rajasekaran, S. Kumar, and J. Weinhold for helpful discussions. We are particularly grateful to R. Krishnamoorti for sending us a copy of his thesis and many stimulating conversations. This work was supported by the Division of Materials Science, Office of Basic Energy Science, U.S. Department of Energy in cooperation with Oak Ridge National Laboratory. Use of the central computing facilities of the UIUC Materials Research Laboratory (via grant number DEFG02-91ER45439) are also acknowledged.

References and Notes

(1) Flory, P. J. *Principles of Polymer Chemistry*; Cornell Univ. Press: Ithaca, 1953.
(2) Krishnamoorti, R. Ph.D. Thesis, Princeton University, 1994.
(3) Graessley, W. W.; Krishnamoorti, R.; Balsara, N. P.; Fetters, L. J.; Lohse, D. J.; Schulz, D. N.; Sissano, J. A. *Macromolecules* **1994**, *27*, 2574, 3073, 3896, and references cited therein.
(4) Krishnamoorti, R.; Graessley, W. W.; Fetters, L. J.; Garner, R. J.; Lohse, D. J. *Macromolecules* **1995**, *28*, 1252.
(5) Graessley, W. W.; Krishnamoorti, R.; Reichart, G. C.; Balsara, N. P.; Fetters, L. J.; Lohse, D. J. *Macromolecules* **1995**, *28*, 1260.
(6) Krishnamoorti, R.; Graessley, W. W.; Balsara, N. P.; Lohse, D. J. *J. Chem. Phys.* **1994**, *100*, 3894.
(7) Balsara, N. P.; Lohse, D. J.; Graessley, W. W.; Krishnamoorti, R. *J. Chem. Phys.* **1994**, *100*, 3905. Graessley, W. W.; Krishnamoorti, R.; Balsara, N. P.; Fetters, L. J.; Schulz, D. N.; Sissano, J. A. *Macromolecules* **1993**, *26*, 1137. Balsara, N. P.; Fetters, L. J.; Hadjicristidis, N.; Lohse, D. J.; Han, C. C.; Graessley, W. W.; Krishnamoorti, R. *Macromolecules* **1992**, *25*, 6137. Walsh, D. J.; Graessley, W. W.; Datta, S.; Lohse, D. J.; Fetters, L. J. *Macromolecules* **1992**, *25*, 5236.
(8) Bates, F. S.; Schultz, M. F.; Rosedale, J. H. *Macromolecules* **1992**, *25*, 5547. Gehlsen, M. D.; Bates, F. S. *Macromolecules* **1994**, *27*, 3611.
(9) Rhee, J.; Crist, B. *Macromolecules* **1991**, *24*, 5663. Nicholson, J. C.; Finerman, T. M.; Crist, B. *Polymer* **1990**, *31*, 2287.
(10) Scheffold, F.; Eiser, E.; Butkowski, A.; Stiener, U.; Klien, J.; Fetters, L. J. *J. Chem. Phys.* **1996**, *104*, 8795.
(11) Schweizer, K. S. *Macromolecules* **1993**, *26*, 6033.
(12) Bates, F. S.; Fredrickson, G. H. *Macromolecules* **1994**, *27*, 1065. Fredrickson, G. H.; Liu, A. J.; Bates, F. S. *Macromolecules* **1994**, *27*, 2503. Fredrickson, G. H.; Liu, A. J.; *J. Polym. Sci. Polym. Phys.* **1995**, *33*, 1203.
(13) Singh, C.; Schweizer, K. S. *J. Chem. Phys.* **1995**, *103*, 5814.
(14) Sanchez, I. C.; Lacombe, R. H. *J. Phys. Chem.* **1976**, *80*, 2352, 2368. Walsh, D. J.; Rostami, S. *Adv. Polym. Sci.* **1985**, *70*, 119.
(15) For recent reviews see: Schweizer, K. S.; Curro, J. G. *Adv. Polym. Sci.* **1994**, *116*, 319. *Adv. Chem. Phys.* **1996**, *98*, Chapter 1.
(16) Singh, C.; Schweizer, K. S. *Macromolecules* **1995**, *28*, 8692.
(17) Schweizer, K. S.; David, E. F.; Singh, C.; Curro, J. G.; Rajasekaran, J. J., *Macromolecules* **1995**, *28*, 1528.
(18) Schweizer, K. S.; Singh, C. *Macromolecules* **1995**, *28*, 2063.
(19) Curro, J. G.; Schweizer, K. S. *Macromolecules* **1990**, *23*, 1402.
(20) Schweizer, K. S. *Macromolecules* **1993**, *26*, 6050.
(21) Schweizer, K. S.; Curro, J. G.; *Chem. Phys.* **1990**, *149*, 105.
(22) Schweizer, K. S.; Yethiraj, A. *J. Chem. Phys.* **1993**, *98*, 9053.
(23) Schweizer, K. S.; Curro, J. G. *Macromolecules* **1988**, *21*, 3070.
(24) Doi, M.; Edwards, S. F. *The Theory of Polymer Dynamics*; Clarendon: Oxford, 1986.
(25) Yethiraj, A.; Schweizer, K. S. *J. Chem. Phys.* **1993**, *98*, 9080.
(26) Honnell, K. G.; Curro, J. G.; Schweizer, K. S. *Macromolecules* **1990**, *23*, 3496.
(27) Weinhold, J. D.; Kumar, S. K.; Singh, C.; Schweizer, K. S. *J. Chem. Phys.* **1995**, *103*, 9460.
(28) Stevenson, C. S.; Curro, J. G.; McCoy, J. D.; Plimpton, S. J. *J. Chem. Phys.* **1995**, *103*, 1208.
(29) Kumar S. K.; Weinhold, J. D. *Phys. Rev. Lett.* **1996**, *77*, 1512.
(30) Rajasekaran, J. J.; Curro, J. G. *J. Chem. Soc. Faraday Trans.* **1995**, *91*, 2427.
(31) Freed, K. F.; Dudowicz, J. *Macromolecules* **1996**, *29*, 625.
(32) Chandler, D.; Andersen, H. C. *J. Chem. Phys.* **1972**, *57*, 1930. Chandler, D. *The Liquid State of Matter;* Montroll, E. W., Lebowitz, J. L., Eds.; North-Holland Publishing Co. Amsterdam, 1982; p 275 and references therein.
(33) Hansen, J. P.; McDonald, I. R. *Theory of Simple Liquids*; Academic: London, 1986.
(34) Flory, P. J. *J. Chem. Phys.* **1949**, *17*, 303.
(35) Ballard, D. G.; Wignall, G. D.; Schelton, *J. Eur. Polym. J.* **1973**, *9*, 965.
(36) Curro, J. G. *Macromolecules* **1994**, *27*, 4665. Yethiraj, A.; Curro, J. G.; Rajasekaran, J. J. *J. Chem. Phys.* **1995**, *103*, 2229.
(37) Singh, C.; Schweizer, K. S. Manuscript in preparation.
(38) Koyama, R. J. *J. Phys. Soc. Jpn.* **1973**, *34*, 1029.
(39) Huber, K.; Burchard, W.; Bantle, W. S. *Polymer* **1987**, *28*, 863.
(40) Ben-Amotz, D.; Willis, K. G. **1993**, *97*, 7736.

(41) Hildebrand, J. H.; Prausnitz, J. M.; Scott, R. L. *Regular and Related Solutions*; Van Nostrand Reinhold Co.: New York, 1970.
(42) Schweizer, K. S.; Curro, J. G. *Phys. Rev. Lett.* **1987**, *58*, 246.
(43) Curro, J. G.; Schweizer, K. S. *J. Chem. Phys.* **1987**, *87*, 1842.
(44) We have not accounted for the overlap correction which stems from the presence of overlaps between nonbonded sites on the same chain. We have also not included the short-range excluded volume interactions between sites separated by two bonds in that the lowest allowable value of θ can be $\theta_0 = 0$. Moreover, we do not calculate $\omega_{13}(r)$ exactly which is the probability density of finding sites 1 and 3 on the same chain separated by a distance r.
(45) Honnell, K. G.; McCoy, J. D.; Curro, J. G.; Schweizer, K. S.; Narten, A. H.; Habenschuss, A. *J. Chem. Phys.* **1991**, *94*, 4659.
(46) David, E. F.; Schweizer, K. S. *Macromolecules* **1997**, submitted.
(47) Chatterjee, A.; Schweizer, K. S. Unpublished calculations.
(48) Han, C.; Boyd, R. *Macromolecules* **1994**, *27*, 5365.
(49) Lohse, D. Private communication, 1995.
(50) Krishnamoorti, R. Private commucation, 1996.
(51) Rajasekaran, J. J.; Curro, J. G.; Honeycutt, J. D. *Macromolecules* **1995**, *28*, 6843.
(52) Curro, J. G. Private communication, 1996.
(53) Gehlsen, M. P.; Rosedale, J. H.; Bates, F. S.; Wignall, G. D.; Hansen, L.; Almadal, K. *Phys. Rev. Lett.* **1992**, *68*, 2452.
(54) Bates, F. S.; Fetters, L. J.; Wignall, G. D. *Macromolecules* **1988**, *21*, 1086. Londano, J. D.; Narten, A. H.; Wignall, G. D.; Honnell, K. G.; Hseib, E. T.; Johnson, T. W.; Bates, F. S. *Macromolecules* **1994**, *27*, 2864.
(55) Barker, J. A.; Henderson, D. *J. Chem. Phys.* **1967**, *47*, 4714.
(56) Curro, J. G.; Yethiraj, A.; Schweizer, K. S.; McCoy, J. D.; Honnell, K. G. *Macromolecules* **1993**, *26*, 2655.
(57) Bates, F. S.; Kumar, A.; Schultz, M. F. *J. Polym. Sci. Polym. Phys.* **1995**, *33*, 1423.
(58) See, for example, Scott, R. L. *J. Polym. Sci.* **1952**, *9*, 423. tenBrinke, G.; Karacz, F. E.; Macknight, W. J. *Macromolecules* **1983**, *16*, 1827.
(59) Schweizer, K. S.; Honnell, K. G.; Curro, J. G. *J. Chem. Phys.* **1992**, *96*, 3211.
(60) Melenkevitz, J.; Curro, J. G.; Schweizer, K. S. *J. Chem. Phys.* **1993**, *99*, 5571; *Macromolecules* **1993**, *26*, 6190.
(61) Grayce, C. J.; Schweizer, K. S. *J. Chem. Phys.* **1994**, *100*, 6846.
(62) Grayce, C. J.; Yethiraj, A.; Schweizer, K. S. *J. Chem. Phys.* **1994**, *100*, 6857; Grayce, C. J.; dePablo, J. J. *Ibid*. **1994**, *101*, 6013.
(63) David, E. F.; Schweizer, K. S. *J. Chem. Soc., Faraday Trans.* **1995**, *91*, 2411.
(64) Singh, C.; Schweizer, K. S. Manuscript in preparation.
(65) Melenkevitz, J.; Curro, J. G. *J. Chem. Phys.* **1997**, *106*, 1216.

MA961332K